

# Hipparcos subdwarf parallaxes - metal-rich clusters and the thick disk

I. Neill Reid

Palomar Observatory, 105-24, California Institute of Technology, Pasadena, CA 91125,  
e-mail: inr@astro.caltech.edu

## ABSTRACT

We have used main-sequence fitting to calibrate the distances to the globular clusters NGC 6397, M5, NGC 288, M71 and 47 Tucanae, matching the cluster photometry against data for subdwarfs with precise Hipparcos parallax measurements and accurate abundance determinations. Both the cluster and subdwarf abundance scales are tied to high-resolution spectroscopic analyses. The distance moduli that we derive for the five clusters are 12.24, 14.52, 15.00, 13.19 and 13.59 magnitudes, with uncertainties of  $\pm 0.15$  magnitudes. As in previous analyses by Reid (1997) and Gratton et al (1997), these distances are higher than those derived in pre-Hipparcos investigations.

The calibrated cluster colour-magnitude diagrams provide fiducial sequences in the  $(M_V, (B-V))$  plane, outlining the distribution expected for stars of a particular abundance. We have combined the photometric data for NGC 6397 ( $[Fe/H]=-1.82$  dex), M5 ( $-1.10$  dex) and 47 Tucanae ( $-0.70$  dex) with the mean colour-magnitude relation delineated by nearby FGK dwarfs to define a reference grid in the  $(M_V, (B-V))$  plane, and we have matched this grid against data for stars drawn from the Lowell proper motion survey, with both Hipparcos astrometry and abundance determinations by Carney et al (1994). Limiting the comparison to non-binaries, there are significantly fewer subluminous stars than expected given the spectroscopic metallicity distribution. Inverting the analysis, this implies a reduction by a factor of three in the proportion of stars contributing to the metal-poor ( $[Fe/H] < -0.4$ ) tail of the Galactic disk. We discuss the implications of these results.

## 1. Introduction

Star clusters, in both the disk and halo of Galaxy, have provided an effective tool for refining stellar evolutionary theory since the original identification of the main-sequence and giant branch by Hertzsprung (1905) and Russell (1911). Given an accurate distance

estimate, each cluster provides a snapshot of the H-R diagram for a given age and metal abundance, mapping not only variations in the overall morphology of the colour-magnitude diagram, but also the evolution of other parameters, such as chromospheric activity, rotation and binary frequency. Once calibrated, the observed distribution of those properties amongst field stars can be used to probe the current characteristics and the star formation history of the local stellar populations.

Clusters also serve as chronometers, marking a lower limit to the age both of individual stellar populations and of the Galaxy as a whole. Few very old open clusters are known, but the oldest, Berkeley 17, with an age of  $12_{-2}^{+3}$  Gyrs (Phelps, 1997), provides an estimate of the time since the onset of star formation within the disk. This is  $\sim 2$  Gyrs older than the age derived from analysis of the white dwarf luminosity function (Oswalt et al, 1996). The lower-abundance globular clusters in the Galactic halo have been identified since the 1950s as fossil remnants from the earliest episodes of Galactic star formation, which occurred during the initial collapse of the protogalaxy (Eggen, Lynden-Bell & Sandage, 1962). Until recently, the 16-20 Gyr age-estimates for the most metal-poor of these halo clusters were at odds with cosmologically-based determinations, which, for conventional cosmologies, indicated ages that were lower by almost a factor of two (Kennicutt et al, 1996). However, improvements in the theoretical treatment of convection, helium diffusion and the equation of state, and a more realistic representation of the population II elemental abundances in stellar models have pushed theoretical H-R diagrams to fainter luminosities and redder colours for a given age (D’Antona et al, 1997). Equally significantly, new parallax data provided by the Hipparcos astrometric satellite (ESA, 1997) have led to accurate distance estimates for a more extensive sample of nearby halo subdwarfs and, as a consequence, improved distance estimates to individual globular clusters. As first pointed out by Reid (1997a - hereinafter paper I), and later corroborated by Gratton et al (1997b), the revised calibration leads to larger distances to the most metal-poor clusters, and hence higher luminosities at the main-sequence turnoff. Combining the theoretical and empirical re-calibrations leads to age estimates of between 11 to 13 Gyrs for the oldest halo clusters, significantly closer to cosmological determinations.

Once distances have been determined, cluster colour-magnitude diagrams can be used to investigate the characteristics of the local stellar population, in particular the abundance distribution. Qualitatively, theoretical models predict that, at fixed helium abundance, main-sequence stars of a given mass become hotter (bluer) and brighter (at least at visual wavelengths) with decreasing abundance. The quantitative variation in colour and luminosity with  $[\text{Fe}/\text{H}]$  is not well-established empirically, since, even post-Hipparcos, local subdwarfs with accurate trigonometric parallaxes are insufficient in number to provide full coverage of the  $(M_V, \text{colour})$  plane. However, cluster colour-magnitude relations, calibrated

by these few fiducial points, can trace, for a specific metal abundance, the position of the main-sequence over a wide range of stellar masses, given the important provisos that the cluster and field-star abundances are tied to a consistent observational calibration, and that there are no systematic difference in secondary parameters, such as the helium abundance.

In this paper we use Hipparcos astrometry of nearby metal-poor stars to determine distances to a number of intermediate-abundance globular clusters, extending to higher abundance the small sample discussed in paper I. Taking the colour-magnitude diagrams of those clusters as references, we deduce the the likely abundance distribution of local proper-motion stars. The paper is organised as follows: section 2 discusses the calibrating observations, comparing abundance determinations from high-resolution and low-resolution spectroscopy of both field subdwarfs and globular cluster giants. Based on this discussion, we define the local subdwarf calibrators; and consider their distribution in the  $(M_V, (B-V))$  colour-magnitude diagram. Section 3 uses these data to estimate distances to intermediate-abundance ( $[M/H] > -1.3$ ) globular clusters. Matching the derived absolute magnitude at the main-sequence turnoff against theoretical predictions, we estimate the age of each cluster. Section 4 discusses the impact of these new results on the distance scale, particularly on measurements of the Solar Radius. The main purpose of the present paper, however, is to use the calibrated cluster data to probe the characteristics of nearby proper-motion stars. Thus, in section 5 we use the  $(M_V, (B-V))$  cluster sequences to define a reference grid against which we can match the observed distribution of proper-motion stars from the Lowell survey (Giclas et al 1970) which have accurate Hipparcos parallax measurements. Many of those stars have either spectroscopic (Carney et al, 1994) or photometric (Sandage & Fouts 1987, Schuster et al, 1993) abundance estimates, and we compare the observed colour-magnitude distribution against that predicted from previous abundance estimates, paying particular attention to the mildly metal-poor stars usually associated with the Galactic thick disk. Section 6 summarises our conclusions.

## 2. The subdwarf sample

### 2.1. Absolute magnitudes

In our initial investigation of the impact of Hipparcos data on the cluster distance scale (paper I), the calibrating subdwarfs were drawn from the subset of the Lowell Observatory proper-motion catalogue which had both Hipparcos astrometry and ground-based spectroscopic and photometric observations by Carney et al (1994) (hereinafter CLLA). We have since been able to expand our reference sample to include a larger number of the classical metal-poor subdwarfs, and data for the 91 stars which form the basis for

the current investigation are listed in Table 1. These stars are chosen as having both high-precision Hipparcos parallax measurements ( $\frac{\sigma_\pi}{\pi}$ ) and abundance estimates based on high-resolution spectroscopy. Where possible, our photometry is taken from CLLA; if such data are not available, we have adopted the V magnitude and (B–V) colour listed in fields 5 and 37, respectively, of the Hipparcos catalogue (ESA, 1997). In some cases, the latter colours differ from the CLLA measurements by several hundredths of a magnitude: for example, HD 19445 is listed as (B–V)=0.49 in the Hipparcos catalogue, as compared with (B–V)=0.45 in CLLA. Given the steep slope of the main sequence, particularly at  $M_V = +5$ , these small differences can have a significant impact on cluster distance estimates derived from main-sequence fitting.

Table 1 lists the absolute magnitudes given by the Hipparcos parallax measurements for each subdwarf. As is now well known, systematic biases can be introduced into a statistical analysis if the calibrating stars have been selected, either implicitly or explicitly, based on the measured parallax,  $\pi$ . Since the number of stars increases with decreasing parallax, observational uncertainties in  $\pi$  lead to the mean distance of a given sample of stars, and hence the mean luminosity, being underestimated. Originally quantified for the case of a uniform spatial distribution by Lutz & Kelker (1973), Hanson (1979) extended the analysis to more general cases, including different spatial distributions and the effects of introducing a magnitude limit. In paper I we adopted Lutz-Kelker corrections based on Hanson’s formalism, matching the parallax distribution of the Lowell stars included in the Hipparcos catalogue,  $N(\pi_0) \propto \pi_0^{-3.4}$ . There are, however, other factors which should be taken into consideration, notably the correlation in the Hipparcos data between the uncertainty in the measured parallax,  $\sigma_\pi$ , and the apparent magnitude (figure 1). The derivation of the individual formal uncertainties is described by Arenou et al (1995), who find that systematic errors in the parallax zeropoint lie at (or below) the 0.1 milliarcsecond (mas) level. The (magnitude,  $\sigma_\pi$ ) correlation is significant in the present context, since the calibration stars are selected based on the parallax precision,  $\frac{\sigma_\pi}{\pi}$ .

We have used Monte Carlo simulations to determine the expected extent of systematic bias in the current sample, generating a sample of ‘stars’ with known properties ( $M_V$ ,  $\pi_0$ , spatial distribution). Adopting a particular distribution of observational uncertainties, we can compare the mean absolute magnitude of a sub-sample, selected based on specific criteria, against the known value. The initial calculation simulates the classic Lutz-Kelker effect. Given an uncertainty of  $\sigma_\pi = \pm 1\text{mas}$  in each parallax measurement, and generating  $10^6$  stars with true distances up to 1 kiloparsec (i.e.  $\pi_0 > 1\text{mas}$ ), figure 2A shows the difference  $\Delta M_V = M_V(\text{true}) - M_V(\text{obs})$  as a function of parallax precision. The turnover in  $\Delta M_V$  at lower parallax precision is due to the distance limit of 1 kiloparsec in the model. We have also plotted the  $n = 4$  and  $n = 3$  versions of Hanson’s Lutz-Kelker

approximation. As noted by Hanson, the  $n = 4$  (uniform distribution) approximation lies slightly below the original Lutz-Kelker calculations.

Figure 2B shows the effect of incorporating a magnitude limit in the  $M(\pi_0) \propto \pi_0^{-4}$  simulation. In this case, we have taken  $M_V=5$  for all stars, with no dispersion, set the magnitude limit at  $V=11.5$ , and, as in figure 2A, adopted an observational error distribution of  $\sigma_\pi = \pm 1\text{mas}$ . The brighter magnitude limit leads to a smaller effective distance limit, fewer stars which can be scattered into the sample from larger distances, and, as a result,  $\Delta M_V$  turns over at a higher parallax precision.

However, figure 1 shows that one cannot characterise the uncertainties in the Hipparcos parallaxes by a single value of  $\sigma_\pi$ . When we adopt a distribution of  $\sigma_\pi$  that is correlated with  $V$  magnitude, as in figure 1, the increased uncertainties in the parallax at fainter magnitudes lead to significantly more bias in the derived mean absolute magnitudes (figure 2C). Allowing for a dispersion in the intrinsic absolute magnitudes has little effect on the bias distribution (figure 2D). However, the bias is dependent on the effective distance limit, and hence on the absolute magnitude of the particular set of stars. Figure 2D plots the  $\Delta M_V$  distributions predicted by our simulations for  $M_V = 3 \pm 0.25$  and  $6 \pm 0.25$ , as well as the  $M_V = 5 \pm 0.25$  model. In each case, the observed bias lies close to the Hanson  $n = 3$  approximation, with the bias ‘saturating’ at the parallax precision which corresponds to the effective distance limit. Hence, for  $\frac{\sigma_\pi}{\pi} > 0.3$ , the absolute magnitudes for the intrinsically brightest stars, which remain in the sample at distances of more than 500 pc, are biased to a greater extent than the  $M_V = 6$  stars.

The present sample, however, is limited to stars with parallaxes measured to a formal precision of at least 15 %. At those high precisions, the predicted bias, at all  $M_V$ , is less than 0.15 magnitudes. Given the results plotted in figure 2D, we have adopted two conventions in the main-sequence fitting in the current paper: first, we use Hanson’s  $n=3$  approximation to derive Lutz-Kelker corrections for the reference stars; and, second, we adopt the Hipparcos parallax measurements directly, applying no LK corrections. In most cases, the higher weight accorded to the higher-precision parallax measurements leads to little difference between the resulting distance estimates. <sup>1</sup>

---

<sup>1</sup> We should emphasise that the distance moduli derived for the metal-poor clusters discussed in paper I are little affected by these considerations. Since the final calibration was based on subdwarfs with parallaxes measured to a precision of 12 % or better, undertaking main-sequence fitting without applying any Lutz-Kelker corrections decreases the resultant best-fit distance moduli by no more than 0.04 magnitude for any cluster.

## 2.2. Abundances and gravities

Theoretical isochrones predict that the absolute magnitudes and colours of main-sequence stars depend on atmospheric composition. Thus, accurate distance estimates can be derived using main-sequence fitting only if the globular clusters and the calibrating subdwarfs are tied to a consistent abundance scale. Abundance measurement in metal-poor stars is complicated by the fact that oxygen and other  $\alpha$ -rich elements (Ne, Mg, Si, S, Ca) are enhanced by +0.2 to +0.3 dex relative to solar ratios (Snedden et al (1991), Sneden et al (1992)) This is a natural consequence of the dominant role played by type II supernovae (massive stars) in chemical evolution during the earliest epochs of star formation (Matteucci & Greggio (1986)). High-resolution spectroscopy, allowing measurement of the line-strengths of individual atomic species, therefore constitutes the preferred method for abundance determination.

Until recently, however, conventional high-resolution spectral analyses have been undertaken for only a restricted number of metal-poor stars. Primarily for that reason, in paper I we adopted cluster and subdwarf abundance calibrations based on other, more widely-applicable techniques. Extensive high-resolution data are now available, however, through Carretta & Gratton’s (1997) analysis of spectroscopy of red giants in 24 clusters, and Gratton et al’s (1997a) re-analysis of high-resolution spectroscopy of nearly 300 field subdwarfs. We have adopted those calibrations in the present analysis, and here we compare the metallicities against our previously-adopted abundance scales.

### 2.2.1. Cluster abundances

The globular cluster metallicities adopted in paper I are taken from the Zinn & West (1984) (ZW85) analysis of large-aperture photometry, where the latter magnitudes are combined to give a number of reddening-independent colour indices which effectively measure the colour of the giant branch and the relative number of blue horizontal branch stars. Both of these properties are correlated, to first order, with abundance. The zeropoint of the abundance scale was set by the few clusters which at that time had high resolution spectroscopic analyses of giant star members. Carretta & Gratton (1997) (CG97), on the other hand, have analysed high resolution ( $R \sim 30,000$ ) spectra of 160 stars in 24 clusters, using the equivalent widths of individual Fe I lines to determine mean  $[\text{Fe}/\text{H}]$  values for each cluster. Their sample includes all of the clusters discussed in section 3, and the same authors have analysed many of the field subdwarfs in our calibrating sample. An important qualification is that, while a consistent set of model atmospheres was used in the cluster-giant spectral-line analysis, the data themselves are drawn from a variety of sources

and do not constitute an homogeneous sample.

CG97 compare their abundance determinations against the ZW85 scale (their figure 5). There is a systematic offset between the two sets of abundance estimates, with the ZW85 scale giving lower metallicities for  $[\text{Fe}/\text{H}] < -1$ . This reflects, to some extent, the higher solar Fe abundance (by +0.15 dex) adopted as standard in the earlier study (see Biemont et al, 1991). The average offset between the CG97 and ZW85 scales is  $\sim 0.15$  dex, but for some intermediate-abundance clusters (such as NGC 288 and M5), the high-resolution abundances are  $\sim 0.3$  dex higher than the old calibration.

### 2.2.2. Subdwarf abundances

A comparison between recent high-resolution spectral analyses of field subdwarfs and the results derived from the CLLA survey reveals systematic differences in the metallicity scales, comparable to those in the cluster comparison. The CLLA calibration is based on echelle spectroscopy, but the practicalities involved in completing a survey of over 1000 stars limited most observations to spectra of relatively low signal-to-noise. Abundances were derived by matching those data against synthetic spectra spanning a range of effective temperature and metallicity (Carney et al, 1987), with the resultant metallicities accurate to 0.1 to 0.2 dex. Stars with high-resolution spectroscopic analyses were used to define the zeropoint of the abundance scale which therefore, like the ZW85 cluster scale, is tied to the older solar iron abundance.

We can compare the CLLA results against data derived from two recent, more conventional analyses of high-resolution spectra: Axer, Fuhrmann & Gehren (1994 - AFG) have derived temperatures, gravities and abundances for 115 metal-poor stars, many of which were identified first in the Lowell survey; and Gratton, Carretta & Castelli (1997a - GCC) have compiled similar data for nearly 300 stars, again analysing both their own spectra and literature equivalent width measurements of Fe I and Fe II lines. We have Hipparcos data for sixty-seven stars from Axer et al (1994) and eighty-seven stars from the Gratton et al (1997a) sample. The two analyses are based on different model atmospheres, with GCC using the Kurucz (1993) calculations, while AFG describe their models as almost identical to those of Kurucz (1979), and use different analysis techniques. These differences lead to systematic offsets in both the effective temperature and the gravity derived for the 22 stars in common between the two samples (figure 3). The abundances, however, are in reasonable agreement, with a mean difference of

$$\Delta[\text{Fe}/\text{H}] = [\text{Fe}/\text{H}]_{\text{GCC}} - [\text{Fe}/\text{H}]_{\text{AFG}} = -0.008 \pm 0.169 \quad (1)$$

There are indications of a systematic offset towards negative residuals (i.e.  $[\text{Fe}/\text{H}]_{AFG}$  higher abundance) for  $[\text{Fe}/\text{H}]_{GCC} < -1.5$ .

Comparing both of these high-resolution studies against the CLLA data shows that the CLLA metallicities tend to be systematically more metal-poor at lower abundances (figure 4). This offset must partly reflect differences between these recent high-resolution analyses and those used to calibrate the CLLA scale. The discrepancy appears less significant for  $[\text{Fe}/\text{H}] > -1$ , but there are relatively few stars in common at those abundances. Generally, the GCC/CLLA residuals show less dispersion, and this may reflect closer agreement between the temperature scales adopted in those analyses. One should also note that the AFG sample includes a larger number of fainter ( $V > 9$ ) Lowell proper-motion stars, while the GCC sample consists primarily of well-known HD subdwarfs. We shall discuss these abundance scales further in section 5.

In this paper we are concerned mainly with the higher-abundance ( $[\text{Fe}/\text{H}] > -1.3$ ) components of the halo and disk. Since there is reasonable agreement between the AFG and GCC analyses at those abundances, our sample of local calibrators is drawn from both compilations. In cases where a star appears in both samples, we have adopted the atmospheric parameters derived by GCC. Data for all of the stars included in our final sample of calibrators are listed in Table 1. There is considerable overlap between these stars and the Hipparcos subdwarfs used as calibrators by Gratton et al (1997b).

### 2.2.3. Abundances and main-sequence fitting

Accurate and self-consistent abundance measurements for the clusters and field stars are required since the validity of the main-sequence fitting technique rests on the assumption that one is matching like with like. Changing either (or both) the cluster or subdwarf abundance scales has two consequences: first, if one limits the comparison to stars within a limited abundance range, a given cluster is matched against a different set of calibrating subdwarfs; second, the  $\delta(B-V)_{[\text{Fe}/\text{H}]}$  colour corrections required to place all subdwarfs on a mono-metallicity sequence are affected. Either adjustment can lead to a change in distance modulus. In the former case, the subdwarf sample is small enough that adding or subtracting one or two stars can change the best-fit distance modulus by  $\sim 0.1 - 0.15$  magnitude.

We can use theoretical isochrones to estimate how differential errors in  $[\text{Fe}/\text{H}]$ , and hence  $\delta(B-V)_{[\text{Fe}/\text{H}]}$ , affect the derived distance modulus. The D’Antona et al (1997) tracks indicate that  $\frac{\partial(B-V)}{\partial[\text{Fe}/\text{H}]} \sim 0.053 \text{ mag dex}^{-1}$  at  $[\text{Fe}/\text{H}] \sim -2$ , but  $\frac{\partial(B-V)}{\partial[\text{Fe}/\text{H}]} \sim 0.143 \text{ mag dex}^{-1}$



at  $[\text{Fe}/\text{H}] \sim -1$ . The slope of the lower main sequence is  $\sim 5$ . Thus, other considerations being equal, distance determinations to metal-poor clusters are less sensitive to changes in the relative abundance scale. A *differential* offset of 0.2 dex between the cluster and field-subdwarf abundance scales leads to a systematic change in the distance modulus of 0.14 mag at  $[\text{Fe}/\text{H}] = -1$  and only 0.05 mag at  $[\text{Fe}/\text{H}] = -2$ . Unfortunately, the majority of metal-poor calibrators with precise parallax measurements tend to be closer to the main-sequence turnoff, where the main-sequence is steeper, compensating to some extent for the reduced metallicity-dependence of the colours.

### 2.3. The HR diagram for metal-poor stars

Figure 5a shows the  $(M_V, (B-V))$  colour-magnitude diagram defined by the 91 stars listed in Table 1. The stars are divided into six subgroups by abundance and two reference sequences are plotted: the mean relation for the nearest stars, derived by Reid & Murray (1993) from ground-based trigonometric parallax data, and the main-sequence relation for the Pleiades, using  $(V, (B-V))$  data from Micela et al (1996) (excluding photometric binaries) and adopting the Hipparcos-based distance modulus of 5.3 (Mermilliod et al, 1997). Figure 5b compares those two sequences against the colour-magnitude distribution described by all stars in the Hipparcos catalogue with  $\pi > 30\text{mas}$  and  $\frac{\sigma_\pi}{\pi} < 0.08$ . The Reid/Murray relation lies toward the lower-luminosity edge of the sequence, as one might expect given that the mean abundance of the local stars is slightly subsolar: Wyse & Gilmore (1995) derive  $\langle [Fe/H] \rangle = -0.14$  dex from 114 G-dwarfs within 25 parsecs of the Sun. Evolutionary effects also obviously lead to the stellar distribution being skewed to redder colours for  $M_V < 4.5$ . That the Pleiades main-sequence lies at lower luminosities is surprising - perhaps the most surprising, and disturbing, result from the Hipparcos mission. While one can account for the discrepancy by invoking a higher helium abundance (Mermilliod et al, 1997), the required abundance may be as high as  $Y=0.35$ , or nearly 40% higher than the helium fraction in the Sun and the Hyades (van Leeuwen & Hansen-Ruiz, 1997). Finally, figure 5c plots the  $(M_V, [\text{Fe}/\text{H}])$  distribution for all of the stars in Table 1.

A number of stars in table 1 are identified as binary or multiple systems, either in the Hipparcos catalogue or by CLLA, but there are only six cases where the companions are both close enough to be unresolved and sufficiently luminous to affect the photometric properties in a significant manner <sup>2</sup>. One such star, unfortunately, is BD +62 268, the only

---

<sup>2</sup>We note that a number of the ‘companions’ listed in the Hipparcos catalogue are line-of-sight optical companions, rather than gravitationally-bound secondaries.

extreme metal-poor star with  $M_V > +6$ . The other stars are HD 7983, 64606, 111971, BD +46 610 and BD +26 2606 (see notes to Table 1). In partial compensation, we have been able to add two wide common proper-motion companions to our calibrating sample: LHS 1279 and HD 158226B.

Of the latter systems, HD 10607(LHS 1281)/LHS 1279 has received less attention. Given the high proper motion ( $0''.57 \text{ yr}^{-1}$ ) and small separation (22 arcseconds), these two stars are very likely to be a physical pair. LHS 1279 does not have extensive radial velocity observations, and there is therefore no conclusive evidence on its multiplicity. Ryan (1992) comments that the pair have discordant photometric parallaxes, but that is on the basis of a linear ( $M_V, (B-V)$ ) relation and on matching both stars against a subdwarf ( $M_V, (R-I)_K$ ) relation. The Hipparcos parallax places HD 10607 ( $M_V=4.06, (V-I)=0.67$ ) slightly above the ( $M_V, (V-I)$ ) relation defined by nearby stars, while, assuming the same distance, LHS 1279 fall  $\sim 0.3$  mag below the relation, at  $M_V=8.17, (V-I)=1.45$ . AFG find  $\log(g)=3.98$  for HD 10607, so the system may consist of a slightly metal-poor subgiant/K-dwarf pair. LHS 1279 has too low an intrinsic luminosity to serve as a distance calibrator in the present study, but, with HST colour-magnitude diagrams extending to close to (even beyond) the hydrogen-burning limit in some clusters, K and M field subdwarfs, such as Kapteyn’s star, LHS 205a or faint halo subdwarfs discovered using the POSS I/II surveys, may well prove useful in future analyses.

AFG also derive a low gravity for the brighter star, HD 158226 (HIC 85378), in the second cpm pair. They estimate the abundance as  $[\text{Fe}/\text{H}]=-0.63$ . This star, also known as G181-47, has a lower-luminosity companion, G181-46, or HIC 85373, which has (within the uncertainties) an identical parallax and, presumably, an identical abundance. Both stars lie well above the mean colour-magnitude relation defined by local dwarfs. (figure 5). G181-46 has a  $(B-V)$  colour of 0.82 mag and  $M_V=5.2$ , and therefore is clearly an unevolved star, lying within the body of the main-sequence defined by the Hipparcos data in figure 5b. Neither component shows velocity variations characteristic of a spectroscopic binary (CLLA). It therefore seems likely that the abundance and gravity of HD 158226 have been underestimated, and that both stars are solar-abundance dwarfs.

Axer et al (1994) identify a significant fraction of the stars in their sample as low-gravity subgiants, and comment that failing to allow adequately for the presence of those stars can bias the conclusions deduced from analysis of large-scale Galactic structure surveys. However, we have already noted that there is a systematic offset between the gravities derived in their study and those calculated by GCC. The Hipparcos parallax data allow us to place individual stars from the two analyses on the colour-magnitude diagram. Figure 6 plots the colour-magnitude diagrams described by all of the AFG and GCC stars with

Hipparcos data. We have divided both samples at  $\log(g) = 4.3$ , plotting the lower-gravity stars as solid symbols. It is clear that while most of the stars classed as subgiants by GCC fall in the expected region of the  $(M_V, (B-V))$  plane, AFG classify a significant number of stars with  $M_V > +5$  as having low gravity. It is extremely unlikely that any of these low-luminosity stars have, in fact, evolved onto the subgiant branch. The hypothesis that a substantial fraction of the Lowell proper-motion stars are subgiants is therefore not supported by the Hipparcos parallax measurements.

There are five stars in the GCC sample which have  $M_V \geq 4.75$ , but which are identified as having low gravity. The bluest of these stars is the metal-poor triple system, BD +26 2606 ( $\log(g) = 4.23$ ), while the four stars lying close to the nearby-star sequence, HIC 51700, 62207, 84862 and 92532, all have abundances between  $-0.38$  and  $-0.51$  and gravities in the range  $4.1 < \log(g) < 4.3$ . HIC 84862 is the nearby star, Gliese 672. If any of these four stars are subgiants, then they are members of a population whose turnoff lies at  $M_V \sim +5$ , implying an age in excess of 20 Gyrs. Lacking any candidate red giant members of such a population, it seems more likely that all four stars are actually near solar-abundance disk dwarfs. This highlights the uncertainties involved in basing age estimates for the local stellar populations on apparently-evolved field stars.

As we noted in paper I, the  $(M_V, (B-V))$  distribution of metal-poor ( $[Fe/H] < -1$ ) subdwarfs with  $M_V > 5$  can be represented by a single main sequence, despite the dispersion in abundance. To some extent, this is expected, given the lower sensitivity of  $(B-V)$  colours to abundance at  $[Fe/H] \sim -2$ . However, the small scatter amongst the  $[Fe/H] < -1.3$  stars in figure 5 is still somewhat surprising. We can quantify this statement by measuring  $\delta M_V$ , the offset in  $M_V$  between the observed position of each star and the corresponding point on the nearby-star sequence. This parameter, subluminosity, can be plotted against abundance and the behaviour compared with that predicted by theoretical models. We have limited our analysis to stars with  $0.55 \leq (B-V) \leq 0.75$ , a colour range that is sufficiently red that theoretical tracks for different abundances are almost parallel, even for old,  $[Fe/H] = -0.7$  clusters such as 47 Tucanae. Figure 7 compares the observations against the predictions of the D’Antona et al (1997) models. The latter are computed for a helium abundance of  $Y=0.23$  at metal abundances  $Z \leq 6 \times 10^{-4}$  and  $Y=0.235$  for higher abundances. While the qualitative agreement is reasonable, the data suggest a less rapid decrease in luminosity than predicted for  $-0.2 < [Fe/H] < -0.6$  and a plateau in  $\delta M_V$  for  $[Fe/H] < -1$ .

In section 5 we will use a variant of figure 7 as a means of probing the abundance distribution amongst Lowell proper-motion stars. This approach inverts the technique usually adopted in stellar population studies. Conventionally, one observes  $V$ ,  $(B-V)$  and  $[Fe/H]$  and uses those data to infer  $M_V$  (as in Laird et al, 1998, for example); we have

observations of  $V$ ,  $(B-V)$  and  $\pi$  (hence  $M_V$ ) and combine those data to infer  $[\text{Fe}/\text{H}]$ . Both techniques rely on there being a one-to-one correlation between position on the HR diagram and  $[\text{Fe}/\text{H}]$ . In both cases, that assumption is complicated by the likely variation in helium abundance over the lifetime of the Galaxy. Theoretical models predict that an increased  $Y$  leads to lower luminosity at fixed  $Z$ , and it is possible that variations in  $Y$  may lead to the increased scatter in  $\delta M_V$  at  $[\text{Fe}/\text{H}] > -1$  in figure 7. Given the difficulties involved in measuring  $Y$  directly in main-sequence stars, the variation is usually presented as a linear increase with increasing  $Z$ , with the latest estimate (Baglin, 1997) indicating that  $\frac{dY}{dZ} \sim 3$ .

In terms of calibrating the effects of changing helium abundance, one can either incorporate an explicit  $\frac{dY}{dZ}$  variation in model isochrone calculations, or, rely on empirical calibration and the assumption that the average trend in  $Y$  with  $Z$  in the calibrators matches that in the programme stars. The latter approach is usually adopted (e.g. Laird et al (1988)), and it is that approach that we follow in section 5. One important point should be emphasised: if variations in  $Y$  are sufficient to invalidate our technique of estimating  $[\text{Fe}/\text{H}]$ , then those same variations also invalidate conventional methods of estimating  $M_V$  based on observations of  $[\text{Fe}/\text{H}]$ .

### 3. Cluster distances by main-sequence fitting

The main purpose of our compiling astrometric and photometric data for nearby metal-poor stars is identifying appropriate sets of subdwarfs which can be used to calibrate the distance moduli of photometrically well-studied globular cluster systems. In such main-sequence fitting analyses, it is customary to emphasise the importance of employing as calibrators only local subdwarfs whose absolute magnitudes are fainter than at least  $M_V = -5.5$ . This criterion is justified on the grounds that one must use stars that are unequivocally on the unevolved main sequence. There are, however, other concerns which should be borne in mind.

First, if one limits the local calibrators to the lowest luminosity subdwarfs, one is also forced to match the observed cluster main-sequence at faint *apparent* magnitudes, where the cluster photometry, particularly the colours, are more liable to significant, and possibly systematic, observational errors. Second, the theoretically-predicted variations in colour due to evolution are small - an age difference of 4 Gyrs leads to a change in the  $(B-V)$  colour at  $M_V = 5$  of barely 0.01 magnitude. The offset between 6 and 10 Gyr isochrones is even smaller. Those uncertainties in colour are minor compared with the problems of matching the line-of-sight reddening, defining compatible cluster and field subdwarf metallicity scales, and ensuring that all of the data are on a self-consistent photometric system. The steep

slope of the main-sequence means that any change in colour is amplified by a factor of at least five in the modulus derived by main-sequence fitting. Thus, an arbitrary change in the line-of-sight reddening of only  $\pm 0.03$  mag corresponds to modifying the best-fit distance modulus by at least 0.1 magnitude.

Finally, increasing age moves a subdwarf to higher luminosities with little change in effective temperature. Thus, the distance of a cluster can be overestimated only if the field subdwarfs are, on average, significantly *older* than the cluster stars, while any field stars that are younger than the cluster will tend to bias the measurement towards too small a distance. Gilmore et al (1995) demonstrate that starcount data offer little evidence for field subdwarfs bluer than the colour of turnoff stars in globulars, suggesting that the majority of the field is at least as old as the clusters. Setting firm limits on the fraction of the halo that is older than the oldest clusters is a more difficult observational task, but there is currently no evidence for a significant pre-cluster population.

Based on these arguments, we include subdwarfs with  $M_V \geq 4.75$  as calibrators in our main-sequence fitting, excluding only stars which are unequivocally subgiants. As in paper I, we calibrate the distances of each cluster by matching the observed  $(V, (B-V))$  fiducial sequence against subdwarfs of the appropriate abundance, generally limiting the calibrators to star within  $\pm 0.25$  dex of the cluster abundance. We have used the isochrones calculated by D’Antona et al (1997) to adjust the  $(B-V)$  colours of the individual subdwarfs to give a mono-metallicity sequence. In each case, we have adjusted the cluster photometry for the line-of-sight reddening, so the offset  $(V_0 - M_V)$  gives a direct estimate of the true distance modulus.

The formal uncertainties in distances derived through main-sequence fitting are difficult to quantify in general terms, since the results are subject not only to the possible presence of systematic errors in the individual abundance and reddening estimates, but also depend on the exact distribution in  $M_V$  of the subdwarfs chosen as calibrators for a particular cluster. Based on both our own calculations using different subdwarf reference stars and on an external comparison with the results derived by Gratton et al (1997b), we estimate that the distance moduli derived for each cluster are uncertain by  $\pm 0.15$  magnitude. Once uniform high-resolution spectroscopic abundance estimates are available for a larger sample of subdwarfs, more accurate distance determinations will become possible.

### 3.1. The extreme metal-poor clusters

While the main focus of the present paper is the intermediate and mildly metal-poor clusters in the Galactic halo, we discuss briefly how adopting the high-resolution abundance calibration affects our estimates of the distance moduli of the lower-abundance clusters, discussed in paper I. There are only two stars in the current sample which are both unambiguously single and which have abundances  $[\text{Fe}/\text{H}] < -1.7$ . These are HD 19445, to which both Gratton et al (1997a) and Axer et al (1994) assign an abundance of  $[\text{Fe}/\text{H}]=-1.89$  and BD +42° 3607, at  $[\text{Fe}/\text{H}]=-2.01$  (Axer et al (1994)). Other recent high-resolution studies derive lower abundances for the former star: -2.2 dex (Magain, 1989); -2.16 (Carney et al, 1997); and -2.0 (R. Peterson, priv. comm.). One could include higher-abundance subdwarfs as calibrators for these extreme clusters, but that requires making significant adjustments to the (B–V) colours. Rather than apply those corrections, which are ill-defined empirically at present, we postpone a direct re-analysis of the most extreme metal-poor clusters until a larger sample of local subdwarfs of comparable abundance have accurate metallicity determinations.

We should, however, comment on the recent study by Pont et al (1997), who have matched the M92 fiducial sequence against seventeen subdwarfs and subgiants with Hipparcos data, deriving a best-fit distance modulus of  $(m-M)_0=14.68$ , almost identical to the pre-Hipparcos analysis. Their calibrating sample includes a larger number of extreme metal-poor ( $-1.8 \leq [Fe/H] \leq -2.6$  on the CLLA scale) stars than in either of the previous analysis (paper I; Gratton et al, 1997b). In their main-sequence fitting, Pont et al give equal weight to each star, whereas we weight the fit linearly by the uncertainty in the parallax. Besides applying classical Lutz-Kelker correction, they have used Monte-Carlo simulations to estimate the biases introduced into a  $\frac{\sigma_\pi}{\pi}$ -limited sample by the increase in  $\sigma_\pi$  with apparent magnitude (figure 1), and the effects of a Malmquist-type bias introduced by observational uncertainties in the abundance estimates. Since the halo abundance distribution peaks at  $[\text{Fe}/\text{H}]\sim -1.5$ , the latter errors will lead to a systematic *underestimation* of the average abundance of stars selected as extreme subdwarfs. Given  $\sigma_{[Fe/H]} \sim 0.15\text{dex}$  (and an intrinsic width,  $\sigma_{Mv}$ , of the main-sequence at given  $[\text{Fe}/\text{H}]$ ), they calculate that the latter two effects combine to give a systematic correction to the subdwarf absolute magnitudes of +0.06 mag (i.e. opposite to classical Lutz-Kelker) at  $[\text{Fe}/\text{H}]=-2.0$  and +0.01 mag at  $[\text{Fe}/\text{H}]=-1.0$ . These corrections are small, and should be smaller in our current analysis, where the abundances are based on high-resolution spectroscopy. More important, the *random* uncertainties in  $[\text{Fe}/\text{H}]$  within a given abundance scale are clearly smaller than the *systematic* differences between different scales.

Pont et al also apply statistical corrections to the absolute magnitudes of the binaries

in their sample, although one should note that their results are not strongly dependent on the inclusion of those stars. They correct each star by +0.375 magnitudes, based on a comparison with the binary fraction in Praesepe. That cluster, however, is sufficiently old ( $\sim 800$  Myrs; Friel, 1995) that mass segregation and evaporation has enhanced the fraction of equal-mass binaries. Given the small sample size, it seems more prudent to simply eliminate known binaries from the calibrating sample, as in our current analysis.

### 3.2. The $[\text{Fe}/\text{H}] \sim -1.6$ clusters

The three intermediate-abundance clusters discussed in paper I (M13, NGC 6752 and M5) are served better by calibrators with high-resolution spectroscopy, and Table 2 lists the distance moduli that we derive for these systems. The cluster fiducial sequences are identical with those used in paper I. Postponing discussion of M5 to the following section, our results are in good agreement both with the distances found in our paper I analysis and by Gratton et al (1997b). The latter is not surprising, given the substantial overlap between the two calibrating samples.

We have added to Table 2 the results of our analysis of one additional intermediate-abundance cluster - NGC 6397, one of the closest globular clusters. Conventional estimates of the distance to NGC 6397 place it at a modulus of between 11.7 and 11.9 magnitudes (Anthony-Twarog, Twarog & Suntzeff, 1992). These estimates, however, are tied primarily to the distance of one 'classical' subdwarf, HD 64090, whose Hipparcos parallax is 20 % smaller than the ground-based measurement cited by Laird, Carney & Latham (1988). The cluster is subject to variable foreground reddening, but there are no indications of an unusually high value of the ratio between total and selective reddening, as is the case with M4 (Liu & Janes, 1990). Vandenberg, Bolte & Stetson (1990 - VBS) estimate a mean differential reddening of  $\delta E_{B-V} = 0.17\text{mag}$  with respect to M92 ( $E_{B-V} = 0.02$ ) and we have adopted that value in the present study.

Figure 8a plots the de-reddened fiducial sequence listed by Buonanno, Corsi & Fusi Pecci (1989) for this cluster, matched against eight subdwarfs from table 1. The best-fit distance modulus is 12.24 magnitudes, even with the application of no Lutz-Kelker corrections. Based on HD 64090 alone, the distance modulus is 12.17 mag. CLLA identify that star as a possible single-lined binary, and Pont et al, using CORAVEL, also suspect the star of low-amplitude velocity variations. However, eliminating HD 64090 from the distance determination increases  $(m-M)_0$  to 12.26 magnitudes. Matching the NGC 6397 upper main-sequence and subgiant branch to an M92 fiducial, VBS derive a difference of 2.17 magnitudes in the apparent distance moduli of the two clusters, implying

$\delta(m - M)_0 = 2.70$ , or  $(m - M)_0 = 14.94$  This takes no account of possible intrinsic differences in the colour-magnitude diagrams due to the lower abundance of M92.

The larger distance that we derive for NGC 6397 is consistent with the de Boer et al (1995) spectroscopic analysis of blue horizontal branch stars in the cluster (Heber et al, 1997). In addition, the observed and predicted magnitudes of the contact variables V7 and V8, discovered by Kaluzny (1997), are in closer agreement for  $(m - M)_0 = 12.24$ , although the two SX Phoenicis stars identified in the same study become significantly more luminous than expected if either is a cluster member.

### 3.3. The $[\text{Fe}/\text{H}] \sim -1$ clusters M5 and NGC 288

The recent photometric study by Sandquist et al (1996), coupled with the extensive monitoring of the cluster RR Lyrae variables by Reid (1996), make M5 one of the best-calibrated globular clusters. Zinn & West (1984) assigned a metallicity of -1.4 to both this cluster and to the more distant NGC 288, but both are assigned significantly higher abundances, of -1.1 and -1.07 respectively, by CG97. Sneden et al's (1992) analysis of the same M5 red giant data leads to a slightly lower abundance of  $[\text{Fe}/\text{H}] = -1.17$  dex. NGC 288 lies towards the South Galactic Pole, and is subject to very little foreground reddening (McFadzean et al (1983), Penny (1984)). Bolte (1992) has obtained deep CCD photometry of the cluster, and has used those data to determine a fiducial main-sequence extending to  $V > 22$ ,  $(B - V) > 0.9$  mag.

Given the similarity in abundance between these two clusters, we follow VBS and use the offset between the two observed fiducial sequences in  $(V, (B - V))$  to estimate the difference in reddening, deriving  $\delta E_{B - V} = 0.01$  magnitude. The line-of-sight reddening towards M5 is generally estimated as  $E_{B - V} = 0.02$  to  $0.03$  mag (paper I). Given the low reddening estimates towards the SGP, we adopt a value of  $E_{B - V} = 0.01$  for NGC 288 and estimate  $E_{B - V} = 0.02$  magnitude for M5. The latter is  $0.01$  mag lower than the value used both in paper I and by Gratton et al (1997b). Matching the reddening-corrected main-sequence against local subdwarfs of the appropriate abundance range gives the best-fit distance moduli listed in Table 2. Note that matching the fiducial sequences gives a difference of  $\delta(m - M) = 0.47$  mag., close to the value derived by independent main-sequence fitting.

Figure 8b plots the calibrated colour-magnitude diagrams of both clusters together with the local subdwarf stars. The excellent agreement between the upper main-sequence, subgiant and giant branches of the two clusters suggests almost identical ages. The offset



of 0.01 to 0.02 magnitude in  $(B-V)$  at fainter magnitudes ( $V > 20.5$  in NGC 288) may reflect either an offset in the photometric calibration, or a bias in the position of the fiducial sequence introduced by the presence of significant numbers of binaries in NGC 288 (Bolte, priv. comm.). This discrepancy underlines our misgivings about limiting main-sequence fitting to stars on the lower main-sequence. Our distance modulus of 15.00 to NGC 288 is  $\sim 0.5$  magnitude higher than previous estimates based on pre-Hipparcos parallaxes for subdwarf calibrators, and  $\sim 0.25$  magnitude higher than the value derived by Gratton et al (1997b). The larger distance is in better accord with spectroscopic analysis of blue horizontal branch stars (Heber et al, 1997). Our M5 result is closer to the  $(m-M)_0=14.49$  derived by Gratton et al (1997b), and the difference can be attributed primarily to the higher reddening adopted in the latter analysis. Finally, we note that VBS group NGC 288 and M5 together with NGC 362 and Palomar 5 in their differential colour-magnitude diagram analysis. The offsets  $\delta E_{B-V}$  and  $\delta V$  that they derive between NGC 288 and NGC 362 and between NGC 362 and Palomar 5 imply distance moduli  $(m-M)_0$  of 15.03 and 17.00 respectively.

### 3.4. The metal-rich clusters 47 Tuc and M71

47 Tucanae (NGC 104) and M71 are the two best-calibrated metal-rich globular clusters amongst the systems studied by Carretta & Gratton (1997). As with M5, Sneden et al (1994) derive a slightly lower abundance for M71,  $[Fe/H]=-0.79$  rather than the  $-0.7$  found by CG97. Hesser et al (1987) undertook an extensive BV photometric study of 47 Tucanae, estimating the line-of-sight reddening as  $E_{B-V}=0.04$  mag, and we have adopted their derivation of the fiducial  $(V, (B-V))$  relation of the cluster stars. M71 was the subject of a detailed investigation by Hodder et al (1992) who present BV photometry to  $V \sim 22$  magnitude, and they estimate the foreground reddening as a substantial  $E_{B-V}=0.28$  magnitude. While the latter factor clearly adds significantly to the uncertainties involved in main-sequence fitting analysis, a comparative study of the offset between the M71 and 47 Tuc colour-magnitude diagrams (*a la mode de* VBS) shows that adopting a differential reddening of  $\delta E_{B-V}=0.24$  mag matches closely the colours at the turnoff.

The conventional estimate of the (true) distance modulus of 47 Tucanae is 13.25 mag (Hesser et al). Gratton et al (1997b) derive a modulus of 13.44 magnitudes, based on five stars with Hipparcos parallax measurements, an estimated reddening of 0.023 mag and a cluster abundance estimate of  $[Fe/H]=-0.73$ . Our best-fit modulus is based on nine stars and is higher by  $\sim 0.13$  magnitude (figure 8c), reflecting primarily the the different line-of-sight reddening adopted in our calculation. Repeating the analysis with  $E_{B-V}=0.023$  mag, we

derive  $(m-M)_0=13.50$  mag (no LK corrections). The remaining 0.06 mag. discrepancy rests with the different sets of subdwarf calibrators used in the two calculations.

### 3.5. Cluster ages and the early history of the Galaxy

The absolute magnitude of stars at the main-sequence turnoff is one of the most frequently-used age indicators for globular (and, indeed, open) clusters. Figure 9 compares the empirical results from the present paper against the ( $M_V^{TO}$ , abundance) isochrones predicted by the D’Antona et al (1997) models. These models use the recent Rogers, Swenson & Iglesias (1996) equation of state; adopt full spectrum turbulence (Mazzitelli et al, 1995), rather than the mixing length approximation, to deal with convection; and adopt the bolometric corrections computed by Kurucz (1993). No oxygen or  $\alpha$ -element enhancements are included in the DCM models, so we follow the Salaris et al (1993) prescription for adjusting the cluster abundances to an ‘effective’  $[Fe/H]$ , assuming  $[\alpha/Fe]=+0.3$  for  $[Fe/H] < -1.2$  and  $[\alpha/Fe]=+0.2$  for NGC 288 and M5.

Our distance scale leads to age estimates of no more than 11 Gyrs for any of the clusters included in the current sample, and decreasing the distance modulus by  $\sim 0.1$  magnitudes, matching the Gratton et al results for the metal-poor clusters, increases the ages to only  $\sim 12.5$  Gyrs on average. Indeed, even adopting  $(m-M)_0 = 14.68$  for M93, the pre-Hipparcos value and 0.25 magnitudes less than our current estimate, gives an age of only 13 Gyrs for that cluster *calibrated by these isochrones*. As emphasised in paper I, a crucial aspect of the D’Antona et al isochrones is that they use the Kurucz (1993) effective temperature/colour transformations, leading to a main-sequence  $\sim 0.05$  magnitudes bluer than the corresponding Vandenberg & Bell (1985) calibration for the same age and abundance. Most importantly, however, the *shape* of the DCM and Vandenberg isochrones differ, particularly at extreme abundances ( $[Fe/H] \sim -2$ ), where matching the lower main-sequence leaves a residual offset of  $\sim 0.05$  magnitudes at the turnoff, with the Vandenberg models bluer. Thus, one is inevitably driven to older ages in analyses based on matching the colours predicted by the Vandenberg isochrones, and to younger ages if one chooses to use the DCM models.

The luminosities predicted by the two sets of models are in closer agreement. However, the Kurucz scale gives  $M_{V\odot} = 4.79$  and  $BC_{\odot} = -0.197$  mag. (D’Antona et al), as compared with the estimates of  $M_{V\odot} = 4.82$  and  $BC_{\odot} = -0.12$  mag derived by Alonso et al (1995). If this difference of 0.1 magnitude in the inferred  $M_{bol\odot}$  can be taken as a simple zeropoint shift, applicable at all abundances, then the implication is that age-estimates based on  $M_V^{TO}$  in the DCM models will be  $\sim 1 - 2$  Gyrs lower than those derived from the Vandenberg

models, which are closer to the Alonso bolometric scale. These *systematic* differences in both the underlying theory, and in transforming between the theoretical and observational planes, are at least as important as the remaining discrepancies in the cluster distance determinations in setting the uncertainties in the age estimates.

The two metal-rich clusters, 47 Tuc and M71, merit special mention. Based on the turnoff luminosities we have inferred for these clusters, both are younger than the average globular system. This is consistent with the horizontal branch morphology, with both clusters possessing only a stubby, red horizontal branch which fails to intersect the instability strip (although 47 Tuc may have one, unusual RR Lyrae member, Carney et al (1993)). Theoretical models of HB stars (Dorman, 1992a,b; Lee & Demarque (1990)) show that the lower the mass of the star, the higher the temperature achieved on the horizontal branch: that is, a red HB is characteristic of a higher mass (by  $\sim 0.05 M_{\odot}$ ), and, presumably, a younger age than the extended blue horizontal branch which is a feature of clusters like NGC 6397 and NGC 288. The models also predict that stars on a 47 Tuc-like red HB are  $\sim 0.1$  to  $0.2$  magnitude more luminous in  $M_V$  than the equivalent-abundance, lower-mass stars which can evolve through the instability strip and become RR Lyraes.

With age estimates for eleven globular clusters, we can combine these data to map out the onset of star formation within the disk and halo populations. Figure 10a plots, as a function of abundance, the ages we deduce for the clusters included in the current paper and in paper I. We also show the age distribution of Galactic open clusters, taking the data from the compilation by Friel (1995), together with the estimated age of the Galactic disk based on the most recent analysis of the white dwarf luminosity function (Oswalt et al, 1996). Figure 10b shows the corresponding diagram if one adopts the globular cluster ages calculated by Chaboyer, Demarque & Sarajedini (1996), based on distance determined by the horizontal-branch luminosity calibration,

$$M_V(HB) = 0.79 + 0.17[Fe/H] \quad (2)$$

Chaboyer et al provide age estimates for a variety of different horizontal-branch calibrations. The calibration we have chosen gives one of the youngest age estimates for M92.

There is an obvious difference in the time spanned by the formation of the halo clusters in the two scenarios outlined in figure 10, with the Chaboyer et al (short distance scale) calibration placing the formation of the oldest clusters (such as M92) over 7 Gyrs before the formation of younger, intermediate-abundance clusters such as M5. More significantly, in the latter scenario, the halo starts forming stars at least 8 Gyrs before the earliest hint of star formation in the disk. Yoshii & Saio (1979) have shown that there are feasible mechanisms which can produce a slower overall collapse of the Galactic halo than the free-fall timescale envisaged originally by Eggen et al (1962), although even their halo

formation occurs over no more than  $\sim 3$  Gyrs. However, their analysis does not provide a mechanism for inhibiting formation of the Galactic disk. Given a crossing time of only a few  $\times 10^8$  years, it seems unlikely that gas clouds can be prevented from colliding and forming stars within a rotating disk until some 8-10 Gyrs after the first halo clusters formed. This is obviously not an issue for the revised globular cluster timescale, where there is at most a gap of 1.5 Gyrs between the onset of star formation in the halo and significant star formation occurring within the Galactic disk.

## 4. Cluster RR Lyraes and the distance scale

### 4.1. The distance to the LMC

One consequence of our revised distance estimates for globular clusters is a new calibration of the absolute magnitude of RR Lyrae stars as a function of abundance. Those variables make an important contribution to the definition of the extragalactic distance scale by providing an independent calibration of the distance to the nearer Local Group galaxies, such as the Magellanic Clouds and M31. In paper I we discussed the impact of the new ( $M_V$ , [Fe/H]) calibration on estimates of the distance to the LMC, and noted that the revised distance modulus of  $18.65 \pm 0.1$  ( $53 \pm 0.7$  kpc) was consistent with the recent re-analysis of both the Cepheid distance scale by Feast & Catchpole (1997) ( $(m-M)_0 = 18.7$ ) and the re-calibration of the mira period-luminosity relation by van Leeuwen et al (1997) ( $(m-M)_0 = 18.54$ ). On the other hand, all of these results are at odds with the most recent analysis of the expanding ring in SN1987A by Gould & Uza (1997), who derive  $(m-M)_0 < 18.44 \pm 0.04$ .<sup>3</sup>

As discussed in paper I, Walker (1992a) has compiled data for RR Lyraes in seven LMC clusters, five of which have abundances close to that of NGC 6397. A direct comparison is complicated by the fact that the Galactic cluster possesses only blue horizontal branch stars and no RR Lyraes ( $\text{HB type} = (B - R)/(B + V + R) = 1$ ). In contrast, the two best-studied LMC clusters, NGC 2257 (Walker, 1989) and NGC 1466 (Walker, 1992b) have a horizontal branch morphology with few red HB stars, but with  $\sim 25\%$  of the stars on the instability strip ( $\text{HB type} \sim 0.75$ ). This suggests that the LMC stars are on average  $\sim 5\%$  more massive than the NGC 6397 HB stars (Dorman (1992b)), and these LMC clusters

---

<sup>3</sup> Note that while Gould & Uza determine the time of maximum light as  $t_+ = 380.7 \pm 6.3$  days, from fitting a cuspy profile to the N III] emission-line data, the actual observed maximum line-flux is  $\sim 410$  days after the supernova implosion. If the latter observation is accurate, the SN1987A distance estimate should be increased by  $\sim 10\%$  to 52 kpc. ( $(m-M)_0 = 18.57$ ).

correspondingly younger. The presence of a more extensive asymptotic giant branch in NGC 1466 supports this hypothesis.

If we assume that the intrinsic luminosities of the horizontal branch stars in NGC 6397 and the LMC clusters are similar, despite the age difference, then we can estimate distance moduli for the latter. Walker lists mean magnitudes for the RR Lyraes in all five  $[\text{Fe}/\text{H}] \sim -1.8$  clusters. The colour-magnitude diagrams for NGC 1466 and NGC 2257 show that the RR Lyraes are  $\sim 0.15$  mag fainter than the mean magnitude of the reddest non-variable stars on the blue horizontal branch. In NGC 6397, the latter stars have  $(B-V)=0.31$ ,  $\langle V \rangle=12.90$ , or  $(B-V)_0=0.12$ ,  $\langle M_V \rangle=+0.1$ , implying that  $[\text{Fe}/\text{H}] \sim -1.8$  RR Lyraes have  $M_V \sim +0.25$ . Averaging the resultant distance moduli for the five LMC clusters gives  $\langle (m - M_0) \rangle = 18.71 \pm 0.06$  mag. This calculation makes no allowance for possible effects due to the depth of the LMC, but if we follow Walker and assume that the clusters lie in the plane defined by the HI disk, then the mean modulus remains unchanged at  $\langle (m - M_0) \rangle = 18.71 \pm 0.07$  mag. Given the morphological differences between NGC 6397 and the LMC clusters, the uncertainty in this estimate is at least  $\pm 0.15$  magnitude. However, the derived distance is more consistent with the longer distance scale than with the SN1987A analysis.

#### 4.2. The distance to the Galactic Centre

In paper I we noted that the absolute magnitude derived for the M5 variables was in poor agreement with results derived from statistical parallax analysis of Solar Neighbourhood RR Lyraes (Layden et al (1996)). Since our cluster abundances were based on the ZW85 scale, the poor agreement might be interpreted as due to a significant difference between the metallicity of M5 and the mean abundance of even the halo field-star sample in the latter analysis. Under the CG97 abundance scale, however, M5 has  $[\text{Fe}/\text{H}]=-1.1$ , and our distance modulus of  $14.52 \pm 0.1$  ( $E_{B-V} = 0.02$ ) implies  $M_V = 0.5 \pm 0.1$  for the cluster RR Lyraes,  $\sim 0.3$  mag brighter than the results derived for field RR Lyraes of the same abundance, and  $\sim 0.15$  mag brighter than the absolute magnitudes predicted for  $[\text{Fe}/\text{H}]=-1$  horizontal branch stars by Caloi et al's (1997) theoretical models. Moreover, under the CG97 calibration M5 has an abundance within 0.1 dex of the average metallicity of the RR Lyraes in the Galactic bulge (Walker & Terndrup, (1991)). Therefore re-calibrating the M5 variables affects directly one method of estimating the distance to the Galactic Centre. Before considering how our current results impinge on this analysis, we review briefly other methods of estimating this quantity.

#### 4.2.1. *The Solar Radius*

Reid (1993) has reviewed the various techniques used to determine  $R_0$ , combining different measurements to derive a “best” estimate of  $R_0=8.0\pm 0.5$  kpc, while Huterer et al (1995) provide a summary of some more recent results. The most direct methods rely on geometry, either direct measurement of the proper motion of the radio source at the Galactic Centre, or the assumption of uniform expansion of water masers. Thus, observations of the  $H_2O$  masers in the Sgr B2 (North) source, which lies  $\sim 300$ pc from the Galactic Centre (Reid et al, 1988), indicate  $R_0=7.1 \pm 1.5$  kpc. Similar analysis of the  $H_2O$  masers in W49 leads to  $R_0=8.1 \pm 1.1$  kpc (Gwinn et al (1992)).

Direct measurement of the proper motion of Sgr A\* yields values of  $(\mu_l, \mu_b) = (-6.55 \pm 0.34, -0.48 \pm 0.12)$  mas yr $^{-1}$ , where the error-bars give the  $2\sigma$  uncertainties (Backer, 1996) Given that this proper motion reflects only the reflex solar motion, then adopting a local rotational velocity of  $\Theta_0 = 220 \pm 20$  kms $^{-1}$  (Brand & Blitz, 1992) and a Solar motion of  $V_\odot = 12$  kms $^{-1}$  with respect to the Local Standard of Rest implies  $R_0=7.5\pm 0.7$  kpc, or  $(m-M)_0=14.38^{+0.19}_{-0.21}$  magnitudes.

Caldwell & Coulson (1987) matched an axisymmetric Galactic rotation model against photometry and radial velocity measurements of field Cepheids to derive an estimate of  $R_0 = 7.8 \pm 0.7$  kpc. Huterer et al (1995) describe other kinematic approaches, combining radial velocity and proper-motion measurements of Bulge giants, but point out that the existence of a bar (Blitz & Spergel, 1991) may well vitiate the assumption of isotropic velocity dispersions which underlies those analyses. Finally, given a flat rotation curve locally,  $R_0$  can be derived from the Oort constants, but current determinations of the latter quantities are sufficiently uncertain to provide only poor constraints.

#### 4.2.2. *RR Lyraes and the distance to the Galactic centre*

Oort & Plaut (1975) carried out the first extensive survey of RR Lyraes in the Galactic Bulge, analysing photographic data for over 1200 variables in several fields to derive  $R_0 = 8. \pm 0.6$  kpc. Most surveys since then have concentrated on the lightly-reddened Baade’s window (see Carney et al, 1995, for a summary). In particular, Walker & Terndrup (1991) combined spectroscopic and visual data for 59 RR Lyraes to estimate a Solar Radius of  $R_0 = 8.2$  kpc for a reddening law where the ratio of total to selective extinction,  $R$ , is 3.1; and  $R_0 = 7.7$  kpc for  $R=3.35$ . Those distances are based on a mean RR Lyrae absolute magnitude of  $\langle M_V \rangle = 0.85$ , consistent with the Carney et al (1992 - CSJ) Baade-Wesselink scale. Adopting  $\langle M_V \rangle = 0.50$ , as indicated by our M5 results, increases the inferred values

of  $R_0$  to 9.6 and 9.0 kpc respectively.

Interstellar reddening is much less of a problem at near-infrared wavelengths, and Fernley et al (1987) demonstrated that there appeared to be little metallicity dependence in the  $(M_K, \log(\text{period}))$  relation. Building on this, Carney et al (1995) used infrared observations of Galactic Centre RR Lyraes to estimate  $R_0 = 7.8$  kpc for an absolute calibration tied to the CSJ calibration. They also calculate results for a relation of the same slope, but scaled to match an LMC distance modulus of 18.5 mag, a zeropoint correction of -0.3 mag. Feast (1997) has argued that the latter adjustment is incorrect, since it is based on a biased derivation of the RR Lyrae  $(M_V, [\text{Fe}/\text{H}])$  relation.<sup>4</sup> Feast derives an  $(M_K, \log(P))$  relation, based on Fernley’s (1994) Baade-Wesselink results for field RR Lyraes, of

$$M_K = -2.566 \log P_0 - 1.034$$

Combined with the Carney et al data on the Bulge RR Lyraes, this leads to an estimate of  $R_0 = 8.1 \pm 0.4$  kpc.

Longmore et al (1990) present K-band observations of eighteen RR Lyraes in M5. Calibrating their absolute magnitudes using our estimate of the distance modulus (14.52 mag), we derive a best-fit period-luminosity relation of

$$M_K = -2.566 \log P_0 - 1.34$$

where we have fixed the slope at the value derived by Feast, and solved only for the zeropoint. This, in turn, implies  $R_0 = 9.3 \pm 0.7$  kpc, or  $(m-M)_0^{GC} = 14.84$ .

#### 4.2.3. Summary

The preceding discussion leads to an apparent paradox. If the Galactic Centre lies at a distance  $R_0 = 8.0$  kpc, then the Bulge RR Lyraes imply  $(m-M)_0 = 14.19$  to M5 and  $\langle M_V(RR) \rangle = 0.85$  at  $[\text{Fe}/\text{H}] = -1.1$ . This is consistent with  $\langle M_V(RR) \rangle$  deduced from both Baade-Wesselink (CSJ) and statistical parallax (Layden et al, 1996) analyses of field RR Lyraes, but disagrees by 0.35 magnitudes with the absolute magnitude of the M5 stars derived on the basis of  $(m-M)_0 = 14.52$ .

On the other hand, the Galactic Centre-based distance to M5 of 6.9 kpc. is significantly shorter than that derived by other studies. Sandquist et al (1996) use pre-Hipparcos

---

<sup>4</sup>Note, however, that Feast & Catchpole’s (1997) re-calibration of the LMC distance based on Hipparcos results leads to a distance modulus of 18.7, in good agreement with our RR Lyrae calculations, and a consequent offset of -0.2 mag. in the absolute magnitudes of the LMC RR Lyraes plotted in Feast’s figure 1.

subdwarf data to derive  $(m-M)_V = 14.41$  to M5 for  $[\text{Fe}/\text{H}] = -1.4$  (increasing the cluster abundance increases the inferred distance modulus), while matching their fiducial sequence to Vandenberg’s enhanced- $[\alpha/\text{Fe}]$  models ( $[\text{Fe}/\text{H}] = -1.3$ ) gives  $(m-M)_V = 14.50$ ; and HD 103095 alone, ( $[\text{Fe}/\text{H}] = -1.22$ ,  $M_V = 6.61 \pm 0.0155$ ,  $(B-V)_{[\text{Fe}/\text{H}] = -1.1} = 0.76$ ), the pivotal subdwarf in pre-Hipparcos cluster main-sequence fitting, leads to a true distance modulus of 14.43 mag ( $E_{B-V} = 0.02$ ) and  $\langle M_V(RR) \rangle = 0.57 \pm 0.1$ , and  $(m-M)_0^{GC} \sim 14.75$  mag.<sup>5</sup>

The paradox exists, however, only if the globular cluster RR Lyraes are identical to both the local field stars and the Galactic Centre variables. That assumption underpins the use of these stars as distance indicators, but is not inviolable. Dorman’s (1992a) models show that the absolute magnitude of the horizontal branch depends on the CNO abundance, with increased abundance leading to higher luminosity. However, even enhancing the CNO fraction by a factor of 60 leads to  $\Delta M_{bol} \sim 1.0$  magnitudes, and there is no evidence for such substantial variations amongst either Bulge stars (McWilliam & Rich, 1994) or local RR Lyraes (Clementini et al, 1995). Indeed, the latter analyses suggest  $[\text{O}/\text{Fe}] \sim +0.7$ , higher than that inferred for cluster stars, while a comparison of the  $(\Delta S, [\text{Fe}/\text{H}])$  relation for field and cluster RR Lyraes suggests that the latter stars have a higher  $\Delta S$  by  $\sim 1$  at  $[\text{Fe}/\text{H}] = -2$ , suggesting weaker calcium lines and lower  $[\alpha/\text{Fe}]$  (Clementini et al, 1995; CG97). Both differences would suggest a luminosity variation in the opposite sense, i.e.  $M_V(\text{cluster}) > M_V(\text{field})$ .

However, there is another possible source of luminosity variation. High-resolution spectroscopy of globular cluster giants, particularly by the Lick-Texas group (Snedden et al, 1994 and refs within) has revealed star-to-star variations in C, N, O, Na, Mg and Al abundances which are both correlated (sometimes anticorrelated, e.g. Na/O) and tend to become more anomalous with increasing luminosity. As summarised by Shetrone (1997), the latter characteristics suggest strongly that mixing within the convective envelope (perhaps drive by rotation) and dredge-up of nucleosynthesis products is the dominant process governing this behaviour, although primordial variations may also contribute in some clusters (e.g.  $\omega$  Cen). Significantly, neither the Na/O anticorrelation nor variation in  $[\text{Al}/\text{Fe}]$  and  $[\text{O}/\text{Fe}]$  has been detected amongst field halo giants (Shetrone, 1997).

Sweigart (1997) has pointed out that if mixing extends to sufficient depth within the envelope to dredge up aluminium, then helium is also dredged up, increasing the helium fraction within the hydrogen envelope. This has important consequences for post-RGB

---

<sup>5</sup>Note that all of these distance estimates are consistent at the  $2\sigma$  level with distance moduli of  $(m-M)_0 \sim 14.3$  for M5 and  $R_0 \sim 8.4$  kpc.



evolution, notably an increased luminosity on the horizontal branch.<sup>6</sup> While Sweigart’s models are limited to a single abundance ( $Z=0.0005$ ,  $[M/H]=-1.6$ ), he estimates the latter variations as  $\Delta \log(L) \sim 1.5 \Delta X_{mix}$ , where  $\Delta X_{mix}$  is the difference in the hydrogen abundance within the envelope and at the base of the dredge-up region. Sweigart suggests that this mechanism could produce the unusually bright RR Lyraes present in some clusters (such as 47 Tuc), while deeper mixing in metal-poor cluster giants might account for both the period-shift effect (Sandage, 1982; 1993a) and the steep ( $M_V$ ,  $[Fe/H]$ ) relation deduced by Sandage (1982, 1993b; and in our paper I) for cluster RR Lyraes. Moreover, a systematic difference of  $\sim 8\%$  in  $\Delta X_{mix}$  between the M5 stars and the average value in the field could account for  $\Delta M_V \sim 0.3$  mag.

Systematic cluster/field differences in horizontal branch absolute magnitudes are not implausible, given the evident scarcity of deep mixing amongst field halo giants, and might stem from environmental (density-related?) variations in the respective star formation sites. Clearly, such variations would have serious consequences for the utility of RR Lyraes as standard candles, although those uncertainties might be minimised by restricting the comparison to variables drawn from similar (present-day) environments, as in the Galactic/LMC cluster variable comparisons in section 5.1. Regardless of the distance scale complications, deep mixing provides a mechanism which might reconcile the independently well-established  $\langle M_V(RR) \rangle$  estimates for the  $[Fe/H]=-1.1$  RR Lyraes in M5 and in the disk and Bulge.

## 5. Probing the abundance distribution of the thick disk

The Hipparcos subdwarf parallax data permit distance determination for globular clusters spanning an abundance range of over 1 dex, from 47 Tucanae at -0.7 dex to NGC 6397 at -1.82 dex. Those clusters define a series of fiducial sequences in the ( $M_V$ ,  $(B-V)$ ) plane which map the location of stars at a number of specific metallicities. Those sequences therefore define a reference grid which can be used to calibrate the relation between subluminality,  $\delta M_V$  (as defined in section 2.3), and abundance. Figure 11 shows the correlation between subluminality and abundance for  $(B-V)$  colours of 0.55, 0.65 and 0.75 magnitude. This is analagous to the variation plotted in figure 7, save that the points at lower abundance are defined by the cluster sequences, rather than by individual stars. Since the former are calibrated by the latter, it is not surprising that the behaviour of  $\delta M_V$  in the two diagrams is very similar. Given the ( $M_V$ ,  $(B-V)$ ) distribution of the  $\pi > 30$  mas

---

<sup>6</sup>The absolute magnitude at the tip of the RGB also increases

Hipparcos stars plotted in figure 5, we have placed the solar metallicity point 0.25 mag above the nearby-star sequence. Our aim is to use the mean relation defined in this figure as an alternative method of examining the abundance distribution of stars in the Lowell proper motion survey, the higher velocity stars in the Solar Neighbourhood.

Based on the dispersion of points in figure 7, we estimate random uncertainties of 0.2 to 0.3 dex in our metallicity estimates. The systematic accuracy of the technique depends on how well the calibrating cluster sequences match the proper motion stars. Of the three fiducial clusters, 47 Tuc is the most important, since we are interested primarily in studying the mildly metal-poor stars in the Galactic disk. Eggen (1990) has pointed out that 47 Tuc giants follow the (CN-strength,  $T_{eff}$ ) relation (traced by the DDO indices  $C_m$  and (42-48)) defined by old disk stars in the Arcturus group, rather than matching the behaviour of members of more metal-poor halo clusters. Moreover, Sneden et al (1994) find that Arcturus itself has a pattern of  $[\alpha/Fe]$  abundance enhancements which closely matches that observed in giants of the 47-Tuc-like cluster, M71. Given these similarities, it is reasonable to take 47 Tuc as representative of the mildly metal-poor old disk. One possible difference might be the helium abundance: if a significant fraction of the field stars with  $[Fe/H] \sim -0.5$  are younger than 47 Tuc, one might expect higher  $Y$ , and a lower luminosity than predicted by the cluster calibrators. In that case, our  $\delta M_V$  calibration will underestimate the metallicity of those stars - i.e. we will overestimate the fraction of mildly metal-poor stars in the sample.

The cluster distance-scale calibration rests on a relatively small number of stars with well-determined abundances. However, we have Hipparcos astrometry for some 2400 stars drawn from the Lowell proper motion survey, with nearly 1700 having parallaxes measured to a precision of better than 10 %. Since the stars are selected from a proper motion sample, the contribution made by higher velocity stars in the Solar Neighbourhood is amplified, and the sample should be well-suited to probing the nature of the thick disk. Before describing our analysis, we summarise the results of previous studies of that population.

### 5.1. The properties of the thick disk

The thick disk population was identified originally by Gilmore & Reid (1983) through analysis of starcount data towards the South Galactic Pole. The number density of stars between 1 and 5 kpc. above the Plane is significantly higher than was expected on the basis of the then-standard old disk/halo galaxy models, and Gilmore & Reid identified the excess stars with a population having a scaleheight of  $\sim 1500$  pc and local density  $\sim 2\%$  of the old disk. More recent analyses, while confirming the complex nature of  $\rho(z)$  (where  $z$  is

height above the Plane), favour a higher local normalisation for the extended component, with values in the range  $\sim 5$  to  $10\%$   $\rho_0(\text{disk})$  (Robin et al, 1996; Reid et al (1996)). The associated density law (exponential or  $\text{sech}^2$ ) is correspondingly steeper to accommodate the observed number densities of stars at moderate heights above the Plane, with typical estimates of an exponential (or equivalent) scaleheight of  $\sim 800$  parsecs. The relatively red colour of the turnoff at  $z \sim 1$  kpc indicates that this is an old population, formed either during the initial stages of dissipational collapse or perhaps as a response to an early merger with a moderately massive companion (Robin et al, 1996). There is, however, no compelling evidence at present to decide whether this component is a separate population, or a subset of the Galactic old disk.

There is also some disagreement over the associated properties - abundance, kinematics - of the thick disk, reflecting the difficulty of unambiguous segregation of those stars from members of the old disk. Most studies have converged on average abundances of  $[\text{Fe}/\text{H}] = -0.5$  to  $-0.7$  dex (Majewski, 1993 and refs within; Gilmore et al (1995); Robin et al, 1996), with a significant low-metallicity tail extending to at least  $[\text{Fe}/\text{H}] \sim -1.6$  (Morrison, 1993; Majewski, 1993; Beers & Sommer-Larsen (1995)). On the other hand, Reid et al (1997) find that spectroscopy of M-dwarfs at  $\sim 2$  kpc above the Plane (i.e. where the thick disk is expected to be dominant) suggests an average abundance closer to solar values. In analyses particularly relevant to the present study, Nissen & Schuster (1991) and Schuster et al (1993) have used accurate Stromgren photometry to derive abundances for over 1200 stars, also drawn primarily (via Sandage & Fouts 1987) from the Lowell survey. They argue that the abundance distribution is well-matched by adding a thick disk component with  $\langle [Fe/H] \rangle = -0.5 \pm 0.1$ ,  $\sigma_{[Fe/H]} = 0.25$  dex to the old disk ( $\langle [Fe/H] \rangle = -0.11$ ,  $\sigma_{[Fe/H]} = 0.16$ ) and halo ( $\langle [Fe/H] \rangle = -1.30$ ,  $\sigma_{[Fe/H]} = 0.60$ ) components. None of these studies find evidence for a significant abundance gradient with height above the Plane.

Kinematically, early studies favoured a population with a substantial ( $\sim 100 \text{ km s}^{-1}$ ) rotational lag with respect to the old disk (Gilmore & Reid (1983); Wyse & Gilmore, (1986)), although this hypothesis was based more on identifying the local metal-rich RR Lyraes as thick disk tracers (based on the inferred  $\sigma_W$ ) than on any direct observations. More recent investigations find a local asymmetric drift of  $\sim 30 \text{ kms}^{-1}$  (Majewski, 1993; Robin et al, 1996), with velocity dispersions significantly higher than those of the old disk. Schuster et al (1993), in particular, propose that the velocity distribution of stars in their sample is well-matched by a three Gaussian distributions, with the thick disk contributing stars with  $\langle V_{rot} \rangle = 180 \pm 50 \text{ kms}^{-1}$  (i.e.  $V = -40 \text{ kms}^{-1}$ ),  $\sigma_V = 50 \text{ kms}^{-1}$  and  $\sigma_W = 46 \text{ kms}^{-1}$ . The old disk and halo are characterised as respectively  $\langle V_{rot} \rangle = 205 \text{ kms}^{-1}$ ,  $\sigma_V = 20 \text{ kms}^{-1}$  and  $\langle V_{rot} \rangle = 20 \text{ kms}^{-1}$ ,  $\sigma_V = 100 \text{ kms}^{-1}$ ,  $\sigma_W = 86 \text{ kms}^{-1}$ . On the other hand, one should note that the last-mentioned analysis does not make quantitative allowance

for selection effects in the sample definition, notably the bias toward higher velocity stars implicit in any proper-motion star sample. Thus, while these data provide evidence that a simple two-component Gaussian (old disk/halo) is not a good match to the local velocity distribution, their model with three *separate* components is consistent with, but not required by, the observations.

Nonetheless, characterising the old disk and thick disk components as kinematically-separable is a useful technique for estimating the completeness of the subset of Lowell proper-motion stars which form the current Hipparcos sample. As described below, the Hipparcos stars were selected from a magnitude-limited subset of the Lowell catalogue,  $V \leq 11$ . However, these stars do not necessarily constitute a magnitude-limited sample - the higher-luminosity stars in the disk populations form proper-motion-limited samples.

In a proper-motion limited sample, the distance limit, and hence the volume surveyed, is set by the average tangential motion. Hence, fractional contribution from a higher-velocity population can be amplified. The amplification factor is reduced if the distance limit is imposed by other factors, such as apparent magnitude or, since we limit our subsequent analysis to stars with  $\frac{\sigma_{\mu}}{\mu} < 0.15$ , parallax precision. In the case of the old disk, the velocity ellipsoid is

$$U_0 = -9, V_0 = -22, W_0 = -7; \sigma_U = 43, \sigma_V = 31, \sigma_W = 25 \text{ kms}^{-1} \quad (3)$$

(Reid et al, 1995), implying an average tangential velocity of  $\langle V_T \rangle = 77 \text{ kms}^{-1}$ . For a proper motion limit of  $\mu > 0''.26 \text{ yr}^{-1}$  (as in the Lowell survey) this corresponds to a median distance of  $r_m \sim 47 \text{ pc}$ , while  $\sim 80\%$  of the sample should lie within  $67 \text{ pc}$  ( $(m-M) \sim 4.1 \text{ mag}$ ). The remaining  $20\%$  of the stars with  $\mu > 0''.26 \text{ yr}^{-1}$  lie at distances extending beyond  $120 \text{ parsecs}$ . Thus, unlike a magnitude- or volume-limited sample, the stellar distribution in a proper-motion-defined sample does not peak at the apparent magnitude limit. For present purposes, we take the  $80\%$ -complete sampling distance,  $r_{80}$ , as the effective distance limit. Since the Hipparcos/Lowell dataset has an *a priori* apparent magnitude limit of  $V \sim 11.0$ , these simulations show that, for disk stars, the transition between a proper-motion limited and magnitude-limited sample occurs at  $M_V \sim 7.0$ .

For the higher-velocity component, Beers & Sommer-Larsen (1995) have used their observations of spectroscopically-selected metal-poor star to estimate the velocity ellipsoid of thick disk stars as

$$U_0 = 0, V_0 = -25, W_0 = 0; \sigma_U = 63, \sigma_V = 42, \sigma_W = 38 \text{ kms}^{-1} \quad (4)$$

values comparable with those derived by Schuster et al (1993). These motions correspond to an average tangential velocity of  $\sim 107 \text{ kms}^{-1}$ ,  $r_m \sim 66 \text{ pc}$  and  $r_{80} \sim 94 \text{ pc}$  ( $(m-M) \sim 5 \text{ mag}$ ).

For an apparent magnitude limit of  $V \sim 11.0$ , these kinematics imply that the sample is proper-motion limited for  $M_V < 6.0$  and magnitude-limited for lower intrinsic luminosities. Within the proper-motion limited régime, the relative number of thick disk to old disk stars in the proper-motion catalogue (given by the ratios of the cube of the tangential velocities) is amplified by a factor of  $\sim 2.7$  over the local space densities. Finally, note that only 20 % of the thick disk stars within the volume defined by  $r < 94$  pc are included in the proper-motion sample.

In contrast, the halo velocity ellipsoid

$$U_0 = 0, V_0 = -236, W_0 = 0; \sigma_U = 153, \sigma_V = 93, \sigma_W = 107 \text{ km s}^{-1} \quad (5)$$

derived by Beers & Sommer-Larsen (1995) implies  $\langle V_T \rangle = 340 \text{ km s}^{-1}$ . Analysis of the LHS catalogue (Reid, 1997b) suggest that the actual average tangential velocity is  $\sim 20\%$  lower, but even in that case,  $r_m \sim 180$  pc, and the effective distance limit in the present analysis is set by parallax precision in the Hipparcos dataset. As a result, halo subdwarfs make a small contribution to the final sample discussed here.

## 5.2. Proper motion samples, Hipparcos and selection effects

The main aim of the current section is to use the Hipparcos parallax measurements to probe the  $(M_V, (B-V))$  distribution of the stars identified by CLLA as members of the Galactic thick disk. It is therefore essential that we establish that the selection effects which are inherent in the definition of the Hipparcos sample do not lead to any systematic bias in our analysis of those stars.

First, both the CLLA sample and the subset of the Hipparcos catalogue discussed here are drawn from the Lowell proper motion survey. The CLLA sample was chosen based on the Lowell colour class (classes 0, +1), supplemented by spectral type information from Luyten’s catalogues, with the aim of identifying F and G stars. (We should note that the Hipparcos sample includes  $\sim 300$  stars with  $(B-V) < 0.75$  which are not included in the CLLA sample, most of which are listed as colour class +2 in the Lowell catalogue). The effective magnitude limit is  $V \sim 14.5$ , although a significant number of fainter stars are included in the sample. There are 1464 stars with UB $V$  data, 1261 of which have spectroscopic abundance estimates.

The Hipparcos dataset of 2400 stars was selected from the  $\sim 3100$  with  $m_{pg} \leq 13$  ( $V \leq 11.5$  for non-degenerates), with the selection based on the scheduling constraints of the astrometric mission, notably meeting the surface density limit of 3 to 4 stars per square degree. The longer observation time required to obtain accurate data for fainter stars also

resulted in the final sample including  $\sim 80\%$  of Lowell catalogue to  $V=10$ , but only  $\sim 50\%$  of the stars between 10th and 11th magnitude. However, the latter restrictions were applied *after* the  $V < 11.5$  sample was defined, and none of the stars was selected for observation based on foreknowledge of parallax, absolute magnitude or abundance. As a result, the stars observed by Hipparcos represent a randomly-selected subset of the Lowell catalogue. Our aim is to define an unbiased sample to match against the CLLA result, and that aim can be achieved by limiting analysis to stars in the proper-motion-limited régime.

Based on the discussion in the previous sub-section, we expect the Lowell/Hipparcos dataset to be proper-motion limited for disk/thick disk dwarfs with  $M_V < 6.0$ . The overwhelming majority of thick disk stars have  $[\text{Fe}/\text{H}] > -1$ , so this absolute magnitude limit corresponds to  $(\text{B}-\text{V}) < 0.70$ . We can test whether our expectations are reasonable by considering the apparent magnitude distribution of stars in the CLLA sample with  $0.55 \leq (\text{B}-\text{V}) \leq 0.70$  (imposing the blue limit to exclude stars near the halo turnoff). Figure 12 plots those data, and shows a clear discontinuity between at  $[\text{Fe}/\text{H}] \sim -1$ . The metal-poor stars span the magnitude range from  $V=9$  to  $\sim 15$ , with the bulk of the stars fainter than 11th magnitude, but only 30 of the 332 stars with  $[\text{Fe}/\text{H}] \geq -1$  have  $V > 11.0$  mag. This is exactly what one would predict given the disk and halo kinematics outlined in the previous section: the relatively bright limiting magnitude of the Hipparcos sample eliminates only a small fraction of the disk/thick disk stars. The Hipparcos data provide a fair sample of the F and G stars in the Galactic disk.

The CLLA sample included a total of 541 stars with  $0.55 \leq (\text{B}-\text{V}) \leq 0.70$ . Table 3 lists the apparent magnitude distribution for all those stars, and for the stars with Hipparcos parallax measurements, in both cases dividing the subsamples at  $[\text{Fe}/\text{H}] = -1$ . Almost 90% of the metal-rich stars with  $V < 10$  have Hipparcos data, but coverage falls to only  $\sim 35\%$  for the fainter stars. However, the broad distance distribution described by proper-motion selected samples mitigates the resultant selection effects. We have used Monte-Carlo simulations to examine how the increased incompleteness at fainter magnitudes affects the detection efficiency as a function of absolute magnitude. We generate a volume-complete sample of stars with  $r < 150$  parsecs,  $+4 \leq M_V \leq 8$ , and kinematics matching those of the thick disk, and identify those with proper motions  $\mu > 0.25$  arcsec yr $^{-1}$ . Our model assumes that 75% of the stars with  $V < 10$  are selected for astrometric observation, but only 30% of those with  $10 < V < 11$ , and none fainter than  $V = 11$ . Thus, our calculation should provide a conservative estimate of the bias against including lower-luminosity stars in the Hipparcos observations. Our results show negligible effects for stars with  $M_V \leq 5$ , while the relative detection efficiency drops to 85% at  $M_V = 5.25 \pm 0.25$ ; 70 % at  $M_V = 5.75$ ; and 50 % at  $M_V = 6.25$ . Based on the 47 Tuc colour-magnitude diagram, we expect thick disk stars with  $(\text{B}-\text{V}) \sim 0.7$  to have absolute magnitude no fainter than  $M_V \sim 6$ . Thus, the thick

disk should be well-represented within this colour-selected subset of CLLA sample with Hipparcos data.

### 5.3. Thick disk stars in the Lowell proper motion catalogue

Carney et al (1989) have proposed that their analysis of the kinematics and abundance distribution of stars in the Lowell catalogue provides evidence for the presence of a kinematically distinct,  $[\text{Fe}/\text{H}] \sim -0.5$  stellar population, which they identify with the thick disk. Our Hipparcos observations provide no new data on the stellar abundance distribution of the latter stars, but we can test whether their distribution in the colour-magnitude diagram matches that predicted on the basis of the  $(M_V, (B-V), [\text{Fe}/\text{H}])$  calibration derived by Laird et al (1988). Inverting the problem, we can use figure 11 to estimate the abundance distribution that is consistent with the observed displacement below the main-sequence.

There are 248 stars in the CLLA sample which colours in the range 0.55 to 0.70 in  $(B-V)$ , spectroscopic abundance estimates and Hipparcos parallaxes measured to a precision of  $\frac{\sigma_\pi}{\pi} \leq 0.15$ . As described in the previous section, these stars provide a fair, unbiased sample of the disk/thick disk stars in the Lowell survey. Figure 13a compares the absolute magnitudes estimated by CLLA for the 192 stars with no evidence of binarity against those derived for the same stars from the Hipparcos astrometry. Twelve stars have  $M_V^{HIP} < 4.2$  and are probably subgiants, and those stars are identified separately in the figure. There is a systematic offset in the sense that the CLLA absolute magnitude estimates are fainter than the directly-determined  $M_V^{HIP}$ . The Hipparcos parallaxes are typically 5 mas (but as much as 13 mas) smaller than those inferred from the  $(M_V, \text{abundance})$  calibration.

Figure 13b matches the observed  $(\delta M_V, [\text{Fe}/\text{H}]_{CLLA})$  distribution against the mean calibration derived from figure 11, limiting the comparison to the 180 single stars in the sample. The sample is dominated by  $[\text{Fe}/\text{H}] < -1$  disk dwarfs, as expected, but the few halo subdwarfs in the sample do lie close to the mean relation. At higher abundances, however, the stars tend to lie above the calibrating relation - that is, there are significantly fewer subluminal stars than one would expect given the number of intermediate-abundance stars identified by CLLA. As a result, if we use our  $(\delta M_V, [\text{Fe}/\text{H}])$  relation to infer the metallicity distribution of the sample, the number of stars in the low-abundance ( $[\text{Fe}/\text{H}] < -0.5$ ) tail of the distribution is reduced significantly. Based on the  $(M_V, (B-V))$  distribution, only  $\sim 15\%$  of the stars have  $-0.3 \leq [\text{Fe}/\text{H}] \leq -1.1$ , while the spectroscopic calibration places approximately 40% of the stars in that abundance range. Since the relative number of the higher-velocity (thick disk) component is amplified by a factor of  $\sim 2.7$  within this proper-motion limited sample (section 5.2), this implies that only  $\sim 5\%$  of a volume-limited

sample of local disk stars fall within this metallicity range.

This result is emphasised in figure 14, where we plot the  $(M_V, (B-V))$  colour-magnitude diagram for all stars in the CLLA sample with  $-0.3 \leq [Fe/H] \leq -0.9$  and with Hipparcos parallaxes measured to a precision of 15% or better. (The data are plotted using Lutz-Kelker corrected  $M_V$ , but those corrections amount to 0.12 magnitudes at most.) As a reference, we plot colour-magnitude relations for NGC 6397, M5 and 47 Tucanae; for the nearby stars; and for the two old, open clusters M67 and NGC 6791. The M67 schematic is derived from Montgomery et al’s (1993) CCD photometry of cluster members (their figure 8), adopting their reddening estimate of  $E_{B-V}=0.05$  mag. With an age of  $\sim 5$  Gyrs (Phelps et al, 1994), M67 has an abundance of  $[Fe/H] \sim -0.09$  dex (Friel (1995)), and matching the upper main-sequence to the nearby-star relation gives  $(m-M)_0=9.6$  mag. NGC 6791, on the other hand, appears to be metal-rich (Kaluzny & Rucinski, 1995), despite being one of the oldest known disk clusters ( $\sim 9 - 10$  Gyrs, Montgomery et al, 1994). The cluster is highly reddened, with estimates ranging from  $E_{B-V}=0.10$  to 0.23 mag (Kaluzny & Rucinski, 1995). Adopting Kaluzny & Rucinski’s preferred value of  $E_{B-V}=0.17$  mag leads to an estimated distance modulus of  $(m-M)_0 = 12.8$  mag if we match the fiducial sequence (from Montgomery et al, 1994) against the Hyades  $(M_V, (B-V))$  relation.

The three sets of panels in figure 14 include 237 of the 441 stars which CLLA identify as having abundances between  $[Fe/H]=-0.3$  and  $-0.9$ . Although the data are subdivided by abundance, there is relatively little difference amongst the three subsets in the observed distribution in the  $(M_V, (B-V))$  plane. To underline that point, the right-hand panels in figure 14 plot the  $(M_V, (B-V))$  distribution predicted for these stars by CLLA. The disparity between the predicted and observed distributions in the two lower-abundance subsets is particularly evident. A modest fraction of those stars are clearly subgiants, but there is also a significant offset between the mean relation defined by the main sequence stars in each subgroup. Almost one-third of the stars in the  $-0.5 > [Fe/H]_{CLLA} > -0.9$  abundance range are identified as binaries, and unresolved binaries clearly can skew the observed distribution to brighter absolute magnitudes. These stars are identified, however, in figure 14, and, while many lie towards the upper edge of the distribution in  $M_V$ , even allowing for an equal-mass companion generally leaves the star closer to the Solar Neighbourhood fiducial than to the 47 Tucanae main-sequence. It is therefore unlikely that the higher average luminosities can be ascribed to this cause. Nor, as we have discussed at length, is the discrepancy likely to reflect biases in the Hipparcos sample selection. We therefore conclude that there is a significant mismatch between the observed and predicted luminosities of the mildly metal-poor stars in the CLLA proper-motion sample.



## 5.4. Discussion

The results plotted in figure 14 can be summarised very simply: there are significantly fewer subluminoous stars than one would expect given the spectroscopic abundance distribution derived by CLLA. We have presented arguments as to why this cannot be ascribed solely to selection effects: the subset of the CLLA sample observed by Hipparcos is a fair sample of the stars in the Lowell survey. One can explain this result in three ways: first, one can postulate that the presence of systematic errors in the Hipparcos parallax measurements. However, those errors must amount to from 4 to 13 mas to account for the substantial differences between the observed and predicted colour-magnitude distributions plotted in figure 14. Errors of this magnitude would have been detected easily in the extensive comparison with previous ground-based observations undertaken by Arenou et al (1995). Indeed, a simple cross-referencing against the full Yale Parallax catalogue (van Altena et al, 1995) would reveal systematics at this level. None such are evident.

The two remaining hypotheses are: that the CLLA abundance analysis systematically underestimates the metallicity of mildly metal-poor stars, placing a disproportionate fraction of the sample in the range  $-0.4 \leq [Fe/H] \leq -1$ ; or, that the abundance estimates are accurate, but there is little correlation between luminosity and metallicity for stars with  $[Fe/H] > -1$  dex. Either conclusion has serious implications: if the latter alternative is correct, then it removes the fundamental assumption in main-sequence fitting (that local subdwarfs lie on the same main-sequence as cluster stars of similar mass and abundance), and casts doubt on the distance moduli derived for metal-rich globulars and metal-poor open clusters; if the former conclusion is correct, then this calls into question the conclusions derived by CLLA from their analysis of the properties of the higher-abundance (non-halo, thick disk) stars in their sample.

We can probe this issue using results from the Schuster et al (1993) uvby survey of Lowell proper motion stars. Schuster & Nissen (1989) use observations of stars with known abundances (based on high-resolution spectroscopic analyses) to calibrate relations between the Stromgren photometric indices ( $(b-y)$ ,  $m_1$ ,  $c_1$ ) and  $[Fe/H]$ . Carney et al (1996) compare their own abundance determinations to the Stromgren scale, and finding a systematic offset, in the sense that  $[Fe/H]_{SN}$  gives higher abundances for mildly metal-poor stars, and an average scatter in the residuals of only  $\pm 0.17$  dex. That comparison, however, is limited to stars from Schuster & Nissen (1988), a sample which consists predominantly of HD stars brighter than 10th magnitude. We have extended the comparison to include the Lowell proper-motion stars observed by Schuster et al.

Figure 15a compares Stromgren-based and CLLA abundance measurements for 420 stars from the Lowell survey. Stars identified as spectroscopic binaries (either confirmed or

suspected) by CLLA, or as having nearby faint companions, are plotted as open symbols. Figure 15b plots the same diagram, but omitting binaries and stars with significant ( $E_{B-V} > 0.02$ ) reddening. We also distinguish between stars brighter and fainter than  $V=10$ . The dispersion of residuals in figure 15b is  $\sigma_{[Fe/H]} \sim \pm 0.2$  dex, increasing to  $\sim \pm 0.3$  dex at lower abundances, although note that (as expected) most of the metal-poor stars have  $V > 10$ . There is a systematic offset of  $\sim 0.2$  dex, independent of abundance and magnitude (fig. 15c), in the sense that the Schuster et al. scale is more metal rich. Figure 15d shows that the residuals also show a strong correlation with (b-y).

Figure 15 also matches the uvby-abundance determinations against the high-resolution analyses of the subdwarf stars listed in Table 1. The comparison with the AFG metallicities shows considerable scatter, perhaps reflecting differences in the effective temperature scales, and a small systematic offset ( $\sim 0.1$  dex) in the sense that  $[Fe/H]_{SN}$  gives lower abundances. The latter offset is larger ( $\sim 0.15$  dex) and more evident in the comparison with the GCC analyses and may well be tied to the revision in the solar iron abundance.<sup>7</sup>

Some 283 of the stars included in the Schuster et al catalogue have Hipparcos parallaxes measured to a precision of 15% or better. However, only thirty-four of those stars have abundances  $[Fe/H]_{SN} < -0.5$ . Figure 16 is analogous to figure 14 in that it compares the observed colour-magnitude diagrams for the uvby sample, segregated by abundance, against fiducial colour-magnitude relations. We also plot subluminosity,  $\delta M_V$ , as a function of  $[Fe/H]_{SN}$  for the 109 stars with  $0.55 \leq (B-V) \leq 0.75$ . The distribution is more symmetric than that described by the CLLA stars in figure 13.

Combining the offsets between the CLLA and Stromgren, and the Stromgren and high-resolution abundance scales leads to the conclusion that there is a systematic offset of  $\sim 0.3$  dex, independent of  $[Fe/H]$ , between the CLLA abundance scale and that defined by the high-resolution analyses which mark the reference scale used in this paper. Clearly, such an offset can account, at least partially, for the systematic discrepancy between the predicted and observed luminosities of the lower-abundance stars in the CLLA sample (figure 14). Any such systematic change in the abundance scale would have clear implications for Galactic structure - notably the population structure in the local disk. Carney et al (1989) have argued for the existence of a discrete thick disk component largely on the basis of a secondary peak in the abundance distribution of the Lowell stars at  $[Fe/H]_{CLLA} \sim -0.4$ . That proposition is supported to some extent by Gilmore et al's (1995) abundance analysis of  $\sim 120$  G-dwarfs at heights of from 1.5 to 3 kpc above the Plane: the

---

<sup>7</sup>Gratton et al (1997c) have re-calibrated the Schuster & Nissen uvby scale using high-resolution data for a large sample of nearby stars.

metallicity distribution shows a broad peak centred at  $[\text{Fe}/\text{H}] \sim -0.6$ . The latter study does not, however, address the issue of the separateness of the parent thick disk population.

The CLLA abundance distribution of the stars plotted in figure 13 does indeed show a subsidiary peak at  $[\text{Fe}/\text{H}] \sim -0.4$ . However, that secondary maximum is not reflected in the  $(M_V, (B-V))$  distribution of those same star. Reversing the usual procedure, and estimating  $[\text{Fe}/\text{H}]$  from the HR diagram position leads to a metallicity distribution centred on  $[\text{Fe}/\text{H}] \sim 0$  and with a relatively small tail to lower abundances. This distribution is more consistent with a continuum than with a superposition of two distinct populations.

Figure 14 implies that stars with  $-0.9 \leq [\text{Fe}/\text{H}]_{\text{CLLA}} \leq -0.3$  all describe essentially the same main sequence. As noted above, one can explain this result either by postulating a weak correlation between  $[\text{Fe}/\text{H}]$  and  $M_V$ , or by a scale error in the abundances. The most effective method of investigating which alternative is preferred would be to obtain high signal-to-noise, high-resolution spectra of Lowell stars with Hipparcos data, choosing the sample to span both a range in  $[\text{Fe}/\text{H}]$  at constant  $M_V$  and constant colour ( $T_{\text{eff}}$ ) and a range in  $M_V$  at constant  $[\text{Fe}/\text{H}]$  and  $(B-V)$ . Differential analysis will reveal whether the different luminosities are due to metallicity differences (i.e. miscalibration of  $[\text{Fe}/\text{H}]_{\text{CLLA}}$ ), or to an intrinsic scatter in the  $(M_V, (B-V))$  relation for stars with the same atmospheric composition.

The revised distances for the Lowell survey stars derived from the Hipparcos astrometry also affect the kinematics deduced by CLLA for the  $[\text{Fe}/\text{H}] > -1$  stars in their sample. CLLA derive their space motions from direct measurements of the radial velocity, and transverse velocities calibrated based on their photometric parallax scale (Laird et al (1988)). The larger distances that we derive from the Hipparcos parallaxes lead to inferred tangential velocities that are higher by up to 30 %. A full re-analysis of the kinematics is outwith the scope of this paper, but, combined with the data plotted in figure 13, the results imply an increased number of high-velocity, near-solar abundance stars.

Finally, only  $\sim 3\%$  of the 2048 Lowell stars with high-precision ( $\frac{\sigma_\pi}{\pi} < 15\%$ ) Hipparcos parallaxes are evolved stars, yet approximately one in five of the stars with  $-0.9 \leq [\text{Fe}/\text{H}] < -0.7$  plotted in figure 14 has an absolute magnitude consistent with its being a subgiant. If those stars have abundances compatible to M71, then the position of the corresponding turnoff of the parent population is  $M_V^{TO} \sim 4.25$ , implying an age of over 14 Gyrs. However, it is also apparent that higher-abundance stars, either main-sequence binaries or  $\sim 5$  Gyr subgiants, can occupy the same position in the  $(M_V, (B-V))$  plane. Given the observed dispersion amongst the low-resolution abundance indicators, it is possible that the evolved stars are closer to solar abundance, and therefore younger than 10 Gyrs. Again, high-resolution analysis of individual stars is required before broad conclusions can be

drawn concerning the global star formation history of the Galaxy.

## 6. Conclusions

We have used main-sequence fitting techniques to determine the distances to globular clusters with abundances in the range  $-0.7 \leq [Fe/H] \leq -1.8$ . The local calibrators are subdwarfs with both accurate metallicities and with accurate Hipparcos parallax measurements. Both the subdwarf and globular cluster abundance scales adopted in this paper are based on conventional analyses of high-resolution spectroscopy. Main-sequence fitting gives results which are in general agreement with the larger distances, and consequent brighter turnoff luminosities, derived in both our previous analysis (Reid (1997a)) and by Gratton et al (1997b). Using models calculated by D’Antona et al (1997) to estimate absolute ages, these data suggest that the time interval between the onset of star formation in the halo and subsequent star formation in the disk was only 1-2 Gyrs. We identify 47 Tucanae and M71 as being significantly younger than the average age of the clusters included in the present sample.

The Carretta & Gratton (1997) abundance scale places M5 at an abundance of -1.1 dex. As a result, there is a conflict between the absolute magnitudes inferred for the cluster RR Lyraes and those derived based on statistical parallax analysis of the field variable in the Solar Neighbourhood. In addition, an  $M_V$  of +0.5 magnitude for  $[Fe/H] \sim -1.1$  RR Lyraes implies a distance of  $\sim 9.3$  kpc to the Galactic Centre, a value over  $2\sigma$  from the currently-preferred value of 8.0 kpc (Reid (1993)). One can account for the discrepancy, however, if the cluster horizontal branch stars have a higher helium abundance in the envelope, as would be expected if dredge-up is responsible for the high  $[Al/Fe]$  ratios observed in the more luminous cluster red giants (Sweigart, 1997). To date, such abundance anomalies have not been detected in field halo RGB stars (Shetrone, 1997).

We have examined the  $(M_V, (B-V))$  distribution of Lowell proper-motion stars with both accurate Hipparcos parallax measurements and with spectroscopic metallicity estimates by Laird et al (1988). Our results show that there are significantly fewer subluminous stars than one would expect given the  $[Fe/H]_{CLLA}$  distribution. Matching the latter abundance estimates against Stromgren photometry suggests that there is a systematic bias in the CLLA scale such that metallicities are underestimated. If we use the cluster  $(M_V, (B-V))$  sequences to calibrate the absolute-magnitude/metallicity distribution of G and early-K dwarfs, then we find that less than 15% of the proper motion stars have abundances below -0.3 dex, half the number with spectroscopic abundance estimates in that same range. We argue that the metallicity distribution inferred from  $\delta M_V$ , the displacement

below the nearby-star main-sequence, is more consistent with a continuum (the disk) than with a combination of two separate populations, the old disk and thick disk.

Finally, we should emphasise that, in contrast to pre-Hipparcos studies, uncertainties in the absolute magnitudes of the calibrating subdwarfs *do not* dominate the error budget in the cluster distance determinations in the current analysis. There are sufficient stars with high-precision parallax measurements to render the results independent of whether systematic Lutz-Kelker corrections are applied or not. The major source of uncertainty in main-sequence fitting now rests in the colour, rather than absolute magnitude, domain. The line-of-sight reddening to each cluster; the ( $T_{eff}$ , colour) calibration of the theoretical isochrones, and hence the mono-metallicity  $\delta(B-V)/\delta([Fe/H])$  corrections; and the metallicity scales adopted for both the clusters and the field subdwarfs, all affect colours (specifically  $(B-V)$ ) to a greater extent they affect than magnitude. The steep slope of the main-sequence guarantees that any systematic error in colour is amplified by a factor of five in distance modulus. The most problematic of these uncertainties is the abundance calibration - a matter underscored by both the contrast between the expected and observed colour-magnitude distribution of what are nominally mildly metal-poor field stars, and the significant scatter in the comparison between low-resolution abundance estimators. Further observations designed to determine the source of this discrepancy, and verify the abundance scale at intermediate abundances, are clearly of the highest priority.

This research made use of the Simbad database, operated at CDS, Strasbourg, France. INR was supported partially by NSF grants AST-9412463 and AST-9318984. Hipparcos data for the subdwarf stars were obtained as part of joint proposals with G. F. Gilmore. The author also acknowledges useful comments by R. Peterson and by the referee, B. Carney.

## REFERENCES

- Alonso, A., Arribas, S. & Martínez-Roger, C. 1995, *A&A*, 297, 197
- Anthony-Twarog, B.J., Twarog, B.,A., & Suntzeff, N.B., 1992, *AJ*, 103, 1264
- Arenou, F., Lindegren, L., Froeschle, M., Gomez, A.E., Turon, C., Perryman, M.A.C. & Wielen, R. 1995, *A&A*, 304, 52
- Axer, M., Fuhrmann, K., & Gehren, T. 1994, *A&A*, 291, 895
- Backer, D.C. 1996, in *IAU Symp. Unsolved Problems of the Milky Way*, eds. L. Blitz & P. Teuben, p. 193
- Baglin, A., 1997, in *First results from Hipparcos and Tycho, Joint Discussion 14, IAU XXIIIrd General Assembly*, ed. C. Turon
- Beers, T.C., & Sommer-Larsen, J. 1995, *ApJS*, 96, 175
- Biemont, E., Baudoux, M., Kurucz, R.L., Ansbacher, W., Pinnington, E.H. 1991, *A&A*, 249, 539
- Blitz, L. & Spergel, D. 1991, *ApJ*, 379, 631
- Bolte, M. 1989, *AJ*, 97, 1688
- Bolte, M. 1992, *ApJS*, 82, 145
- Bolte, M., & Hogan, C.J. 1995, *Nature*, 376, 399
- Brand, J. & Blitz, L. 1992, *A&A*, 275, 67
- Buonanno, R., Corsi, C.E., & Fusi Pecci, F. 1989, *A&A*, 216, 80
- Caldwell, J.A.R. & Coulson, I.M. 1987, *AJ*, 93, 1090
- Caloi, V., D'Antona, F., Mazzitelli, I. 1997, *A&A*, 320, 823
- Carretta, E. & Gratton, R.G. 1997, *A&AS*, 121, 95
- Carney, B.W., Fulbright, J.P., Terndrup, D.W. Suntzeff, N.B., Walker, A.R. 1995, *AJ*, 110, 1674
- Carney, B.W., Laird, J.B., Latham, D.W., Kurucz, R.L. 1987 *AJ*, 94, 1066
- Carney, B.W., Latham, D.W., & Laird, J.B. 1989, *AJ*, 97, 423

- Carney, B.W., Latham, D.W., Laird, J.B., & Aguilar, L.A. 1994, AJ, 107, 2240 (CLLA)
- Carney, B.W., Laird, J.B., Latham, D.W. & Aguilar, L.A. 1996, AJ, 112, 668
- Carney, B.W., Storm, J. & Jones, R.V. 1993, ApJ, 386, 663 (CSJ)
- Carney, B.W., Storm, J. & Williams, C. 1993, PASP, 105, 294
- Carney, B.W., Wright, J.S., Sneden, C., Laird, J.B., Aguilar, L.A., Latham, D.W. 1997 AJ, 114, 363
- Chaboyer, B., Demarque, P., Sarajedini, A. 1996, ApJ, 459, 558
- Clementini, G., Carretta, E., Gratton, R., Merighi, R., Mould, J.R., & McCarthy, J.K. 1995, AJ, 110, 2319
- D’Antona, F., Caloi, V., & Mazzitelli, I. 1997, ApJ, 477, 519 (DCM)
- de Boer, K.S., Schmidt, J.H.K., & Heber, U. 1995, A&A, 303, 95
- Dorman, B. 1992a, ApJS, 80, 701
- Dorman, B. 1992b, ApJS, 81, 221
- ESA, 1997, The Hipparcos catalogue, ESA SP-1200
- Eggen, O.J., Lynden-Bell, D., Sandage, A.R. 1962, ApJ, 136, 748
- Eggen, O.J. 1990, AJ, 100, 1159
- Feast, M.W. 1997, MNRAS, 284, 761
- Feast, M.W., Catchpole, R.W. 1997, MNRAS, 286, L1
- Fernley, J. 1994, A&A, 284, L16
- Fernley, J.A., Longmore, A.J., Jameson, R.F., Watson, F.G & Wesselink, T., 1987, MNRAS, 226, 927
- Friel, E.D. 1995, ARA&A, 33, 381
- Giclas, H.L., Burnham, R. Jr., & Thomas, N.G. 1971, Lowell Proper Motion Survey (Lowell Observatory, Flagstaff, AZ)
- Gilmore, G.F. & Reid, I.N. 1983, MNRAS, 202, 1025

- Gilmore, G.F., Wyse, R.F.G., Jones, J.B. 1995, *AJ*, 109, 1095
- Gould, A. & Uza, O. 1997, preprint
- Gratton, R.G., Carretta, E., & Castelli, F. 1997, *A&A*, 314, 191
- Gratton, R.G., Fusi Pecci, F., Carretta, E., Clementini, G., Corsi, C.E., & Lattanzi, M. 1997, *ApJ*, in press
- Gratton, R.G., Carretta, E., Clementini, G., Sneden, C. 1997, *Hipparcos Venice Symposium*, ESA SP-402
- Gwinn, C.R., Moran, J.M. & Reid, M.J. 1992, *ApJ*, 393, 149
- Hanson, R.B. 1979, *MNRAS*, 186, 875
- Heber, U., Moehler, S., Reid, I.N. 1997, *Hipparcos Venice Symposium*, ESA SP-402
- Hertzprung, E. 1905, *Zeitschrift für wissenschaftliche Photographie*, 3, 429
- Hesser, J.E., Harris, W.E., Vandenberg, D.A., Allwright, J.W.B., Shott, P., & Stetson, P.B. 1987, *PASP*, 99, 739
- Hodder, P.J.C., Nemeč, J.M., Richer, H.B., Fahlman, G.G. 1992, *AJ*, 103, 460
- Huterer, D., Sasselov, D.D., Schechter, P.L. 1995, *AJ*, 110, 2705
- Kaluzny, J. 1997, *A&AS*, 122, 1
- Kaluzny, J. & Rucinski, S.M. 1995, *A&AS*, 114, 1
- Kennicutt, R.C., Freedman, W.L. & Mould, J.R. 1995, *AJ*, 110, 1476
- Kurucz, R.L. 1979, *ApJS*, 40, 1
- Kurucz, R. L., 1993, *ATLAS9 Stellar Atmosphere Programs and 2 kms<sup>-1</sup> Grid*, (Kurucz CD-ROM No. 13)
- Laird, J.B., Carney, B.W., & Latham, D.W. 1988, *AJ*, 95, 1843
- Layden, A.C., Hanson, R.B., Hawley, S.L., Klemola, A.R., & Hanley, C.J. 1996, *AJ*, 112, 2110
- Lee, Y.W. & Demarque, P. 1990, *ApJS*, 73, 709
- Liu, T. & Janes, K.A. 1990, *ApJ*, 360, 561



- Longmore, A.J., Dixon, R., Skillen, I., Jameson, R.F., Fernley, J.A. 1990, MNRAS, 247, 684
- Lutz, T.E., & Kelker, D.H. 1973, PASP, 85, 573
- McFadzean, A.D., Hilditch, R.W., & Hill, G. 1983, MNRAS, 205, 525
- McWilliam, A., Rich, R.M. 1994, ApJS, 91, 749
- Magain, P. 1989, A&A, 209, 211
- Majewski, S.R. 1993, ARA&A, 31, 575
- Matteucci, F., Greggio, L. 1986, A&A, 154, 279
- Mazzitelli, I., D'Antona, F. & Caloi, V. 1995, A&A, 302, 382
- Mermilliod, J.-C., Turon, C., Robichon, N., Arenou, F. 1997, Hipparcos Venice Symposium, ESA SP-402
- Micela, G., Sciortino, A., Kashyap, V., Harnden, F.R., Rosner, R. 1996, ApJS, 102, 75
- Montgomery, K.A., Marschall, L.A., Janes, K.A. 1993, AJ, 106, 181
- Montgomery, K.A., Janes, K.A., Phelps, R.L. 1994, AJ, 108, 585
- Morrison, H.L. 1993, AJ, 105, 539
- Nissen, P.E., Schuster, W.J. 1991, A&A, 251, 457
- Oort, J.H. & Plaut, L. 1975, A&A, 41, 71
- Oswalt, T.D., Smith, J.A., Wood, M.A., & Hintzen, P., 1996, Nature, 382, 692
- Penny, A.J. 1984 MNRAS, 208, 559
- Phelps, R.L., Janes, K.A., Montgomery, K.A. 1994, AJ, 107, 1079
- Phelps, R.L., 1997, ApJ, 483, 826
- Pont, F., Mayor, M., Turon, C., Vandenberg, D.A. 1997, A&A, in press
- Reid, I.N. 1996, MNRAS, 278, 367
- Reid, I.N. 1997a, AJ, 114, 161 (paper I)
- Reid, I.N. 1997b, Proper Motions and Galactic Astronomy, ASP Conf. Ser. , ed. R. Humphreys

- Reid, I.N., Hawley, S.L., Gizis, J.E. 1995 AJ, 110, 1838
- Reid, I.N. & Majewski, S.R. 1993 ApJ, 409, 635
- Reid, I.N., & Murray, C.A. 1993, AJ, 103, 514
- Reid, I.N., Yan, L., Majewski, S.R., Thompson, I., Smail, I. 1996 AJ, 112, 1472
- Reid, I.N., Gizis, J.E., Cohen, J.G., Pahre, M., Hogg, D.W., Cowie, L., Hu, E., Songaila, A. 1997, PASP,
- Reid, M.J. 1993, ARA&A, 31, 345
- Reid, M.J., Schneps, M.H., Morn, J.M., Gwinn, C.R., Genzel, R., Downes, D., Romang, B. 1988, ApJ, 330, 809
- Robin, A.C., Haywood, M., Crézé, M., Ohja, D.K., Bienaymé, O. 1996, A&A, 305, 125
- Rogers, F.J., Swenson, F.J., & Iglesias, C.A. 1996, ApJ, 456, 902
- Russell, H.N. 1911, Carnegie Inst. Wash. Publ., nr. 147
- Ryan, S.G. 1992, AJ, 104, 1144
- Salaris, M., Straniero, O., & Chieffi, A. 1993, ApJ, 414, 580
- Sandage, A. 1982, ApJ, 252, 553
- Sandage, A. 1993a, AJ, 106, 687
- Sandage, A. 1993b, AJ, 106, 703
- Sandage, A. & Fouts, G. 1987, AJ, 93, 74
- Sandquist, E.L., Bolte, M., Stetson, P.B., & Hesser, J.E. 1996, ApJ, 470, 910
- Schuster, W.J., Nissen, P.E., 1988, A&AS, 73, 225
- Schuster, W.J., Nissen, P.E., 1989, A&A, 221, 65
- Schuster, W.J., Parrao, L., Contreras Martínez, M.E. 1993, A&AS, 97, 951
- Shetrone, M. 1997, AJ, 112, 1517
- Snedden, C., Kraft, R.P., Prosser, C.F. & Langer, G.E. 1991, AJ, 102, 2001
- Snedden, C., Kraft, R.P., Prosser, C.F. & Langer, G.E. 1992, AJ, 104, 2121

- Snedden, C., Kraft, R.P., Langer, G.E. & Prosser, C.F., 1994, *AJ*, 107, 1773
- Sweigart, A.V., 1997, in proceedings of the Third Conference on Faint Blue Stars, ed. A.G.D. Philip (Davis Philip, Schenectady)
- van Altena, W.F., Trueng-liang Lee, J., Hoffleit, D., 1995, *The General Catalogue of Trigonometric Stellar Parallaxes* (Newhaven: Yale Univ. Obs.)
- Vandenberg, D.A., & Bell, R.A. 1985, *ApJS*, 58, 561
- Vandenberg, D.A., Bolte, M., & Stetson, P.B. 1990, *AJ*, 100, 445 (VBS)
- van Leeuwen, F., Feast, M.W., Whitelock, P.A., Yudin, B. 1997, *MNRAS*, 287, 955
- van Leeuwen, F., Hansen-Ruiz, C.S. 1997. *Hipparcos Venice Symposium*, ESA SP-402
- Walker, A.R. 1989, *AJ*, 98,2086
- Walker, A.R. 1992a, *ApJ*, 390, L81
- Walker, A.R. 1992b, *AJ*, 104, 1395
- Walker, A.R., & Terndrup, D.M. 1991, *ApJ*, 378, 119
- Wyse, R.F.G., & Gilmore, G.F. 1986, *AJ*, 91, 855
- Wyse, R.F.G., & Gilmore, G.F. 1995, *AJ*, 110, 2771
- Yoshii, Y., Saio, H. 1979, *PASJ*, 31, 339
- Zinn, R., & West, M., 1984, *ApJS*, 55, 45

FIGURE CAPTIONS

Fig. 1.— The formal uncertainties in the Hipparcos parallax measurements, plotted as a function of apparent magnitude.

Fig. 2.— Monte-Carlo simulations of Lutz-Kelker corrections. *A*: The bias in  $M_V$  as a function of parallax precision for a uniformly-distributed sample with  $r < 1000$  pc,  $M_V = 5$  and  $\sigma_\pi = 1$  mas. The solid and dotted lines show the Hanson (1979)  $n=4$  (uniform density) and  $n=3$  approximations. *B*: the same simulation, but with a magnitude limit added at  $V=11.5$ . *C*: the effect of allowing  $\sigma_\pi$  to vary with apparent magnitude, as in figure 1. *D*: a dispersion of  $\sigma_M = 0.25$  mag has been included. We plot the predicted bias for  $M_V = +6$  (triangles) and  $M_V = +3$  (open circles) besides the  $M_V = +5$  (crosses) prediction

Fig. 3.— A comparison between the abundances, gravities and temperatures calculated by Gratton et al (1997a) and Axer et al (1994) from analysis of high-resolution spectroscopic data.

Fig. 4.— The Carney et al (1994) abundance determinations compared against metallicities derived by Axer et al (1994) and Gratton et al (1997a).

Fig. 5.— a: The  $(M_V, (B-V))$  colour-magnitude diagram described by the stars listed in Table 1. The smaller solid dots mark the position of stars within 25 parsecs of the Sun. The solid line marks a nearby-star main-sequence relation derived by Reid & Murray (1993), and the dotted line outlines the Pleiades main-sequence relation for  $(m-M)=5.3$ . No Lutz-Kelker corrections have been applied to the subdwarf data. b: The two fiducial sequences plotted in figure 5a compared to the  $(M_V, (B-V))$  distribution of Hipparcos stars with  $\pi > 30$  mas and with  $\frac{\sigma_\pi}{\pi} < 0.08$ . c: the abundance distribution of the calibrating subdwarfs. The five binaries excluded from the main-sequence fitting analysis are marked as open squares.

Fig. 6.— Stars classified as dwarfs and subgiants in the high-resolution analyses. In each case, stars with  $\log(g) < 4.3$  are plotted as filled symbols. It is clear that the Axer et al (1994) analysis misclassifies a significant number of *bona-fide* dwarfs as subgiants

Fig. 7.— The correlation between subluminality,  $\delta M_V$ , the distance that a star falls below the Reid & Murray (1993) nearby-star relation, and abundance for stars with  $0.55 < (B-V) < 0.75$ . The dotted line shows the dependence predicted by the D’Antona et al (1997) isochrones at  $(B-V)=0.60$ .

Fig. 8.— Main-sequence fitting distance determinations for the five clusters listed in Table

2. In each case the observed parameters for the subdwarfs are plotted as open squares, while the corrected positions (used in the fitting) are plotted as solid squares. The solid line marks the Reid & Murray (1993) nearby-star relation.

Fig. 9.— The observed main-sequence turnoff absolute magnitudes plotted against the predictions of the D’Antona et al (1997) models. Since the models include no  $[\alpha/\text{Fe}]$  enhancement, the cluster abundances have been adjusted by +0.2 for  $[\text{Fe}/\text{H}] < -1.2$  and by +0.15 at higher abundance (Salaris et al, 1993).

Fig. 10.— A comparison between the star-formation history of the Galaxy deduced by Chaboyer et al (1996), based on globular cluster distances derived using the cited horizontal branch ( $M_V$ ,  $[\text{Fe}/\text{H}]$ ) relation, and the halo cluster ages deduced from figure 11. The crosses plot the ages of Galactic open clusters (from Friel (1995)), while the box (WD) marks the age estimated for the Galactic disk from analysis of the white dwarf luminosity function (Oswalt et al (1996)).

Fig. 11.— The dependence of main-sequence luminosity on abundance defined by the calibrated sequences of the globular clusters 47 Tucanae, M5 and NGC 6397. As in figure 8, the dotted line shows the dependence predicted by the D’Antona et al (1997) models at  $(B-V)=0.6$ , while the empirical relations are plotted for three colours.

Fig. 12.— The apparent magnitude distribution of stars in the full CLLA sample with colours in the range  $0.55 \leq (B-V) \leq 0.70$ . Note the distinctly different magnitude distributions of the disk stars, at  $[\text{Fe}/\text{H}] \leq -1$ , and the higher-velocity dispersion, metal-poor halo subdwarfs.

Fig. 13.— A comparison between the predicted and observed absolute magnitudes for 225 single stars with  $0.55 \leq (B - V) \leq 0.70$ , and both CLLA abundance data and Hipparcos parallaxes measured to a precision of  $\frac{\sigma_\pi}{\pi} \leq 0.15$ . The top panel plots, as a function of  $[\text{Fe}/\text{H}]_{\text{CLLA}}$ , the difference between the CLLA predicted  $M_V$  and the Hipparcos measurements. Probable subgiants are plotted as open triangles. The middle panel matches  $\delta M_V$  (from  $M_V(\text{Hip})$ ) against the mean relation from figure 11. The final panel compares the abundance distribution that we infer from the single-star  $\delta M_V$  distribution (excluding subgiants) against that derived directly from the CLLA spectroscopy.

Fig. 14.— The  $(M_V, (B-V))$  colour magnitude diagrams described by stars from the CLLA sample with both spectroscopic abundances in the range -0.3 to -0.9 dex and Hipparcos parallaxes with  $\frac{\sigma_\pi}{\pi} \leq 0.15$ . The data are subdivided into three abundance subgroups. In each case, the left hand panel plots the Hipparcos-calibrated absolute magnitudes, while the right-hand panel plots the predicted distribution from CLLA. The Solar Neighbourhood main-sequence is shown as a solid line, and the three globular cluster sequences plotted

are for 47 Tucanae (solid line); M5 (dotted line); and NGC 6397 (dashed line). The M67 ([Fe/H]=-0.09, 5 Gyrs) and NGC 6791 ([Fe/H]=+0.2, 9-10 Gyrs) colour-magnitude relations are also plotted for the higher-abundance stars. The encircled points denote stars identified by CLLA as definite or suspected spectroscopic binaries

Fig. 15.— a: A comparison between the abundances derived by Schuster et al (1993) for Lowell proper-motion stars and the CLLA metallicities. Open triangles mark stars identified as definite or possible spectroscopic binaries (CLLA) or stars with nearby faint companions which might affect the Stromgren colours; b) as in a), but omitting all binaries and stars with  $E_{B-V} > 0.02$  mag. Open squares denote stars brighter than  $V=9$  magnitude. The subsequent four plots are restricted to these stars. c) the residuals plotted as a function of apparent magnitude - most of the highly-discrepant points lie at  $V > 9$ th magnitude; d) residuals as a function of  $(b-y)$  - it is clear that there is a correlation with colour; e) the abundance comparison between the Stromgren photometric calibration and the Gratton et al (1997) high-resolution analyses; f) the Schuster et al abundances compared to the metallicities derived by Axer et al (1994).

Fig. 16.— The  $(M_V, (B-V))$  distribution of the 283 Schuster et al stars with high-precision parallaxes. The three stars plotted as crosses in the lowest-abundance subsample ( $-0.5 > [Fe/H] > -1$ ) have abundances  $[Fe/H] < -0.7$ . We also plot the  $(\delta M_V, [Fe/H])$  distribution for the 109 stars with  $0.55 \leq (B-V) \leq 0.75$ .

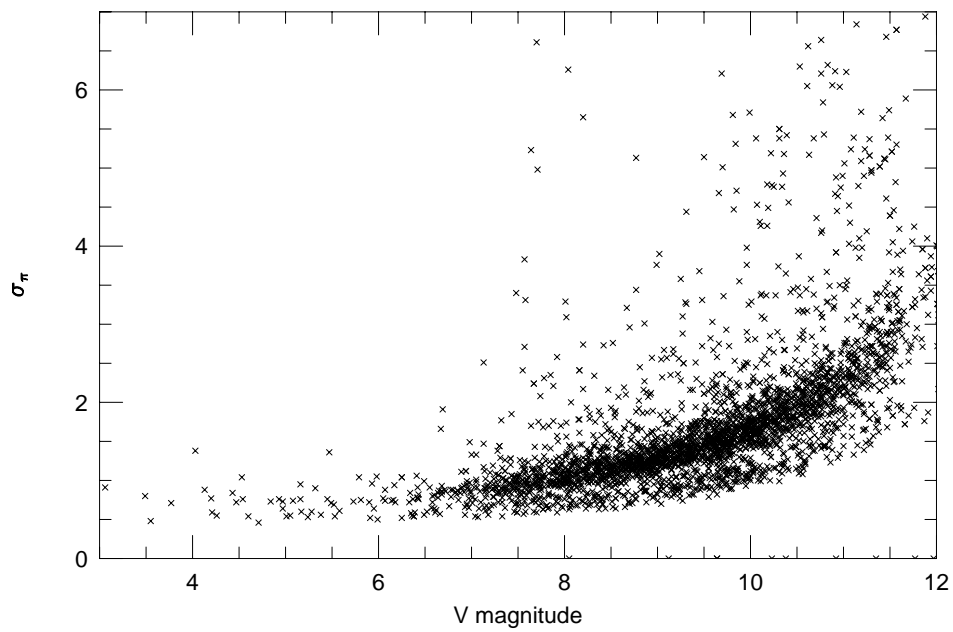


Fig. 1.—

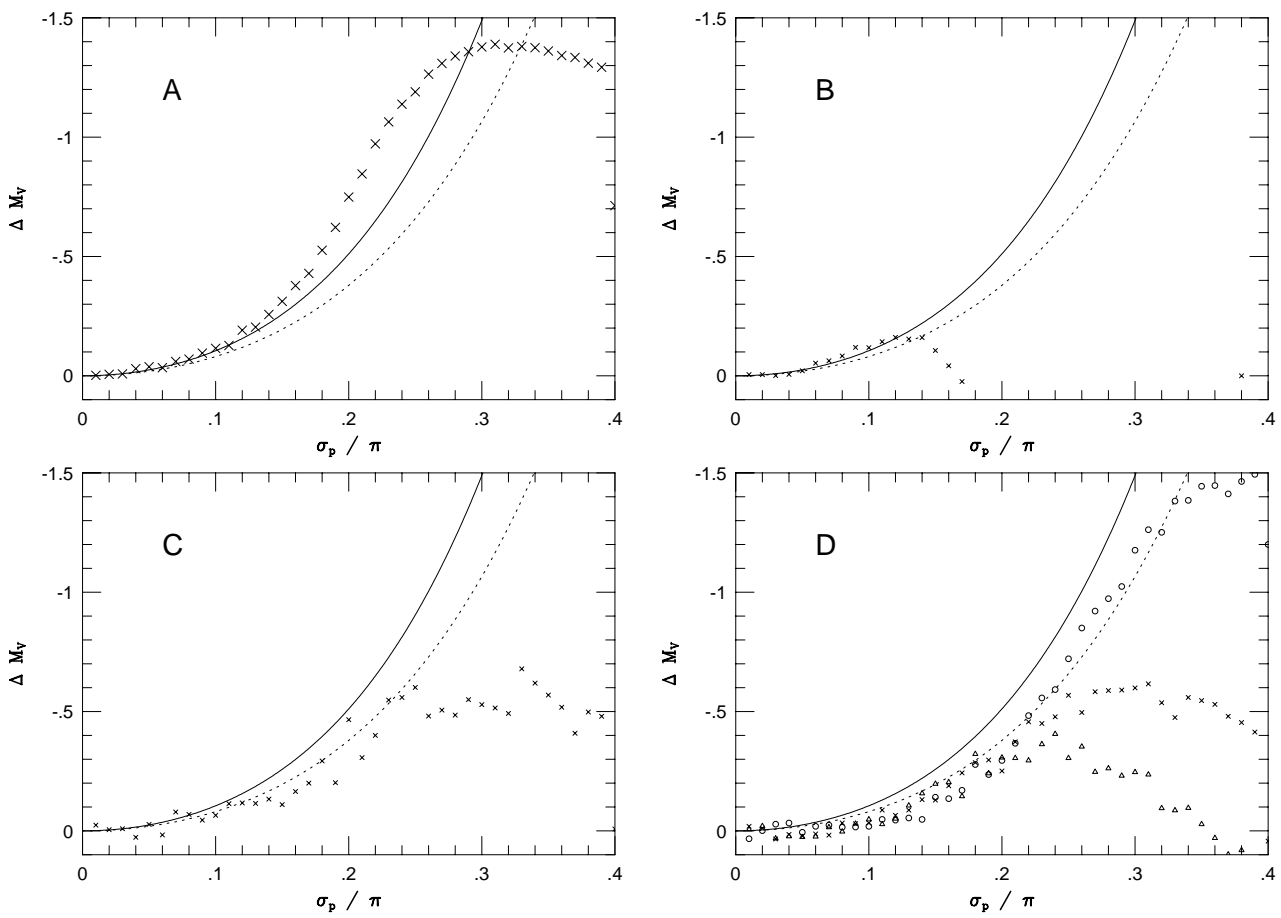


Fig. 2.—



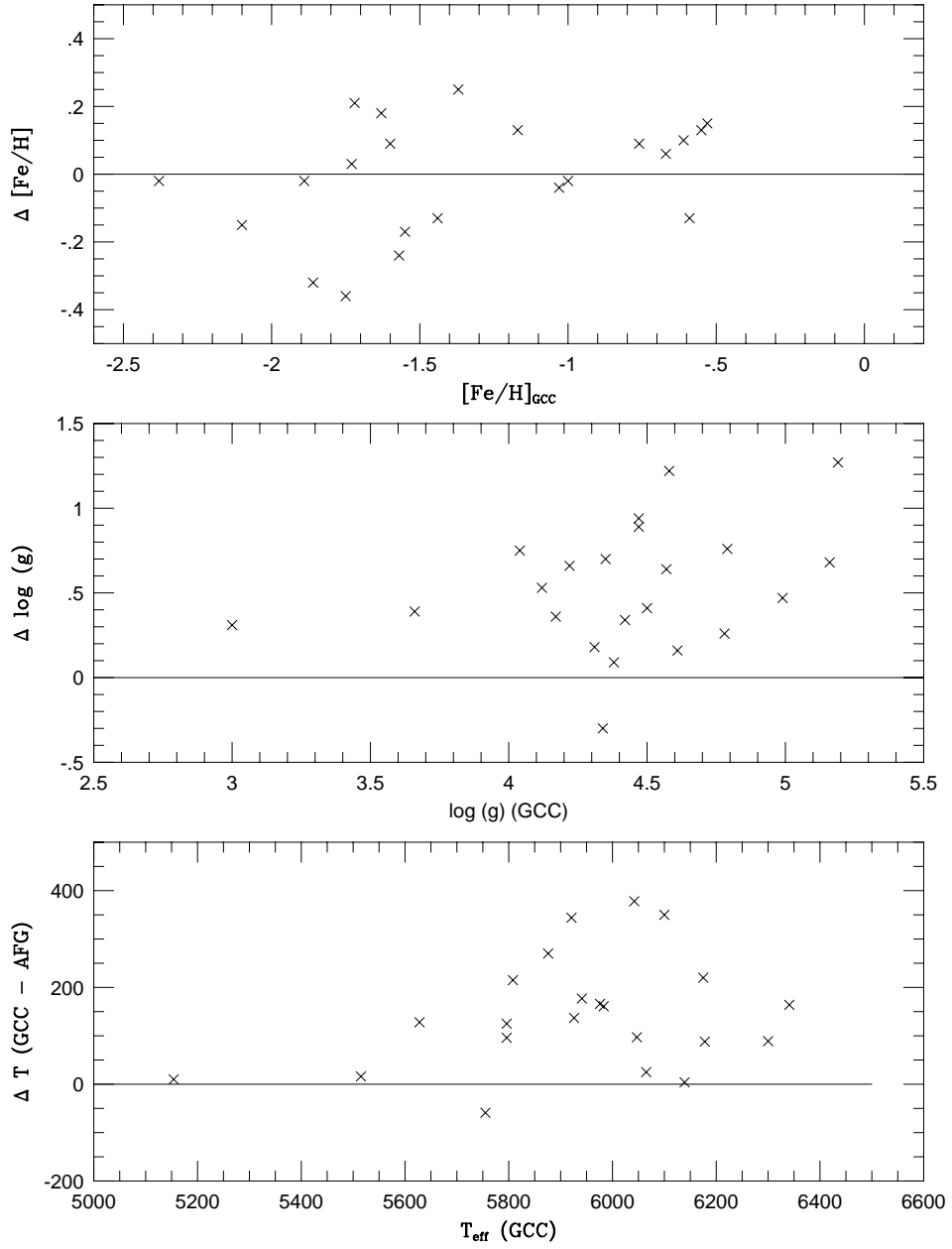


Fig. 3.—

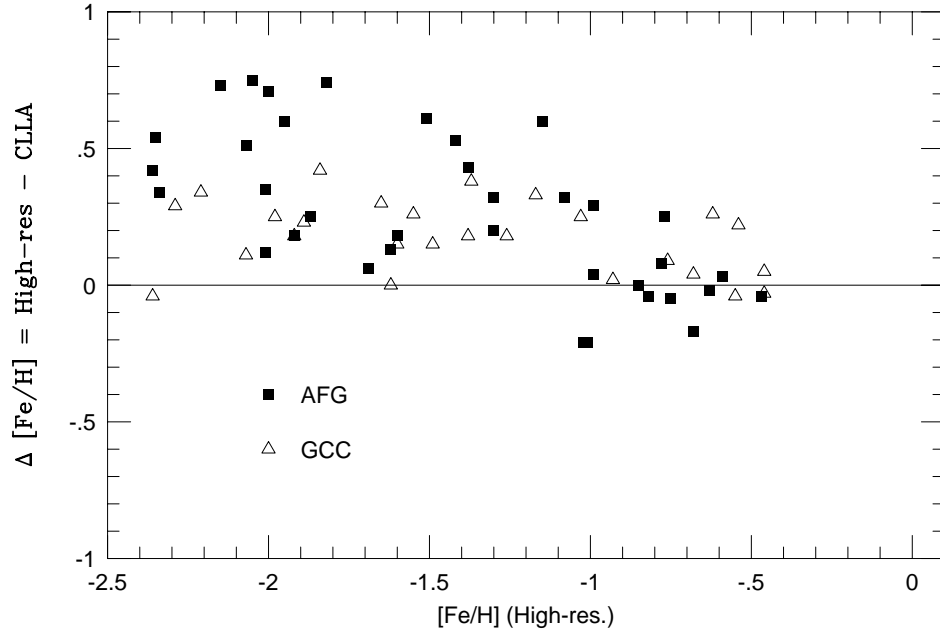


Fig. 4.—

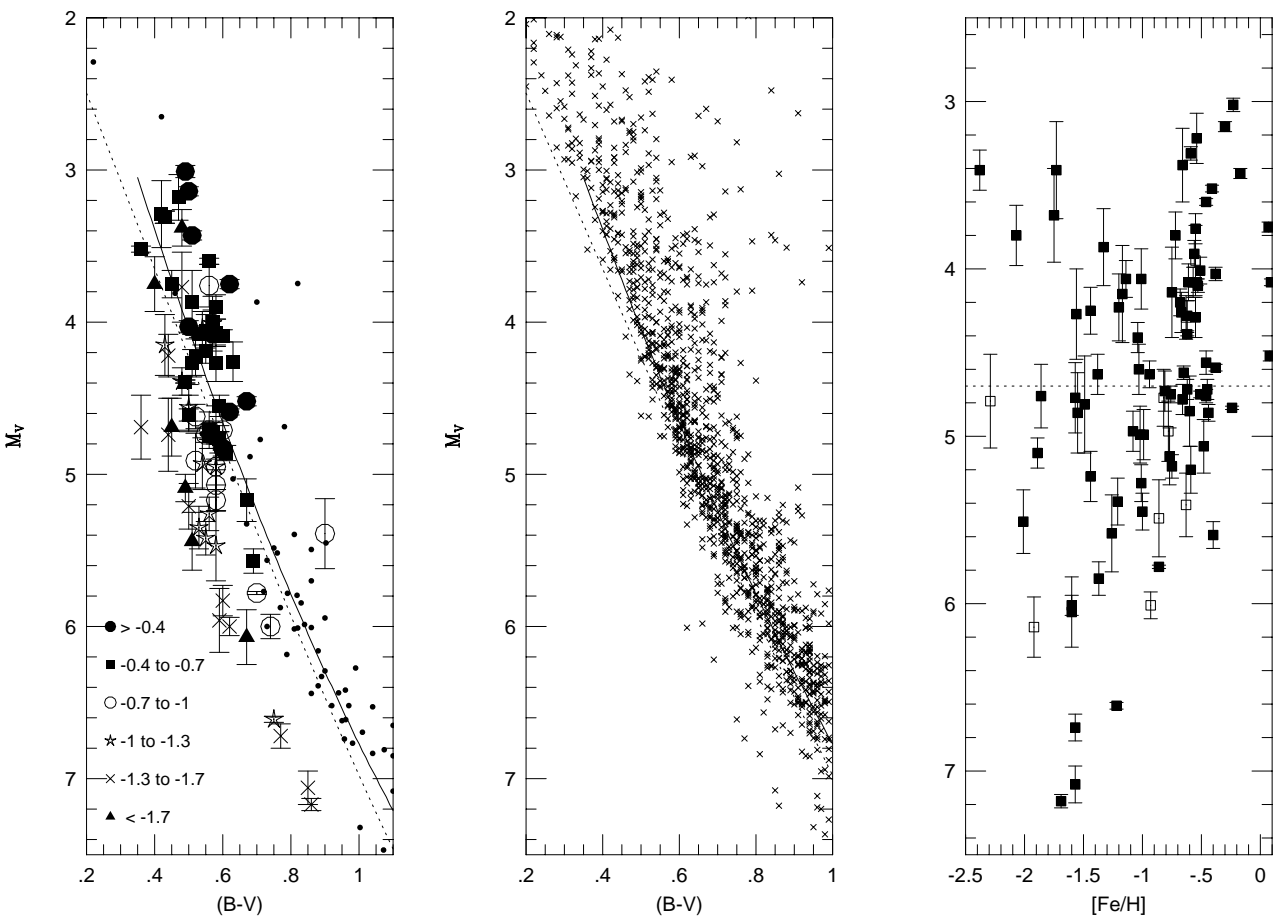


Fig. 5.—

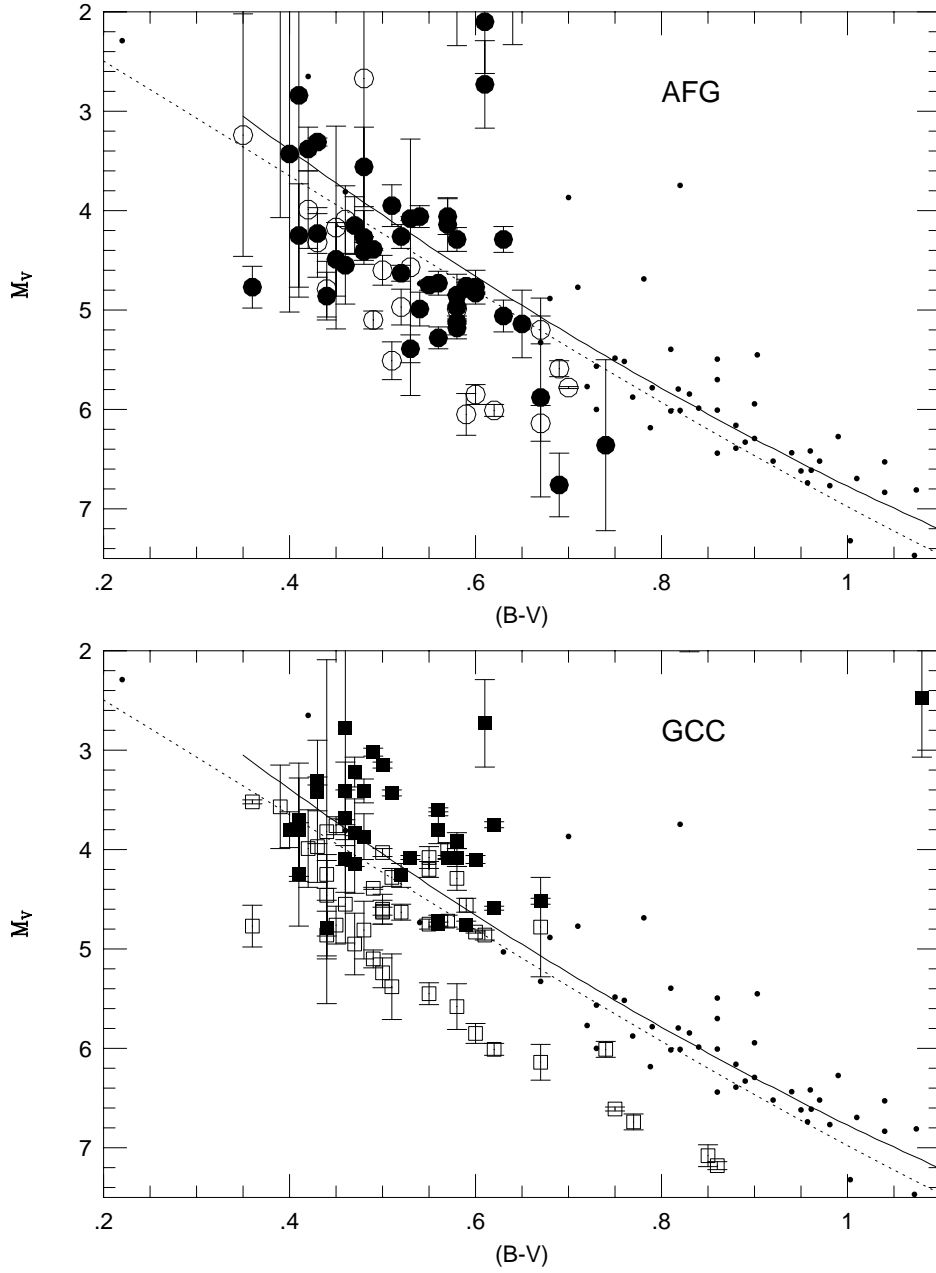


Fig. 6.—

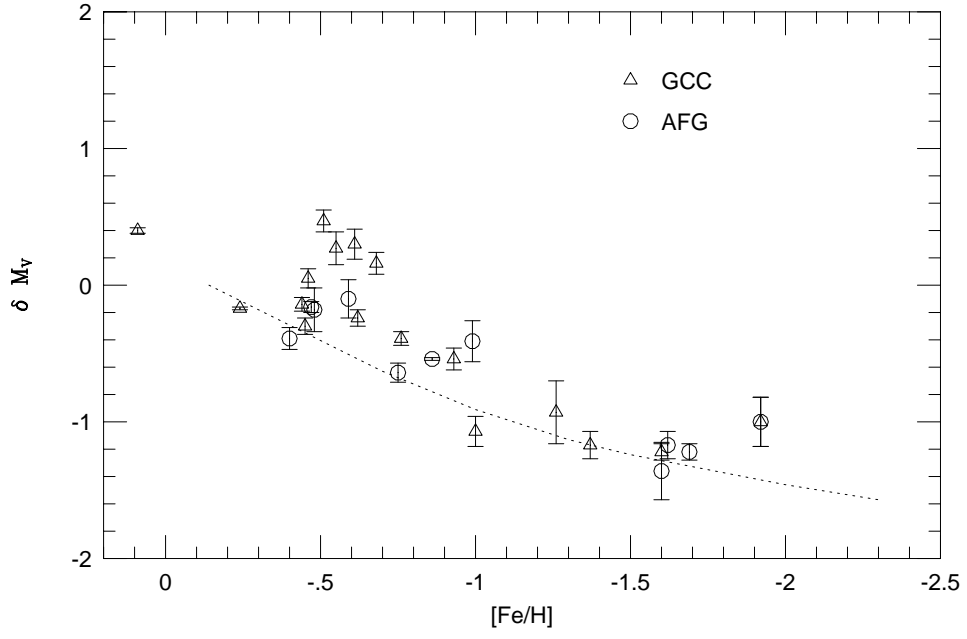


Fig. 7.—

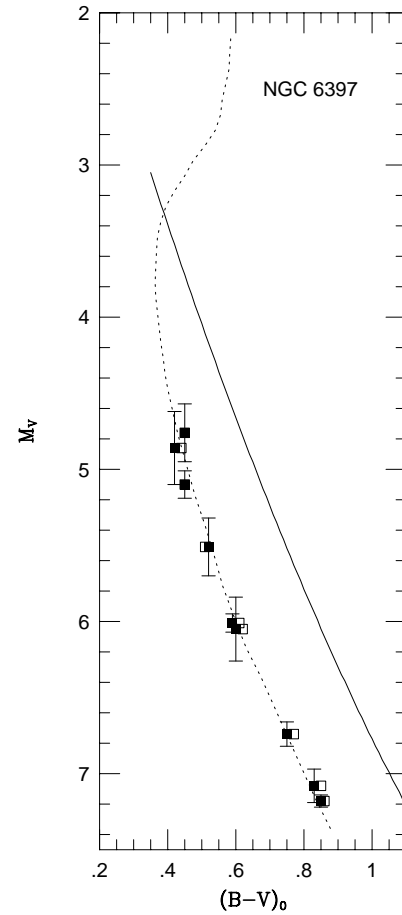
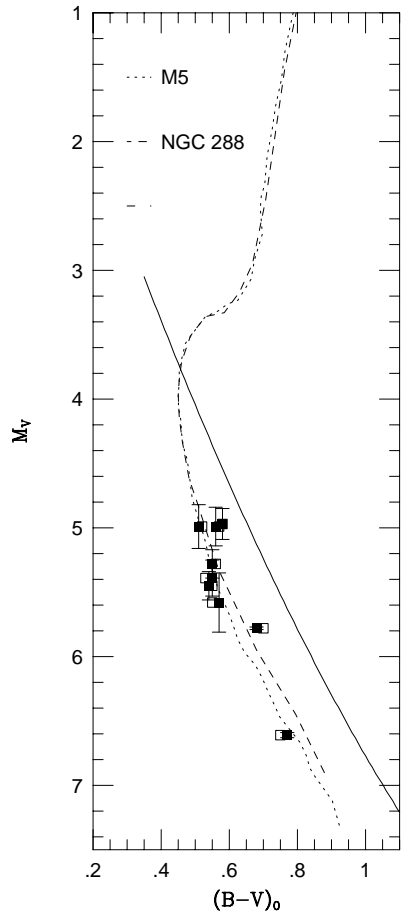
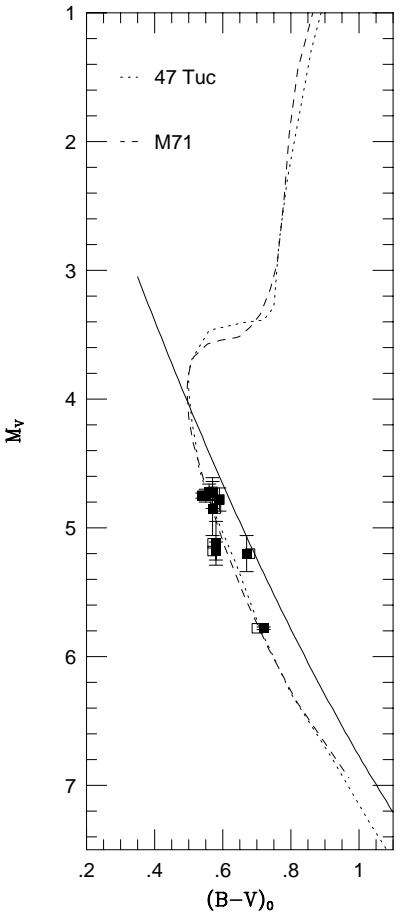


Fig. 8.—

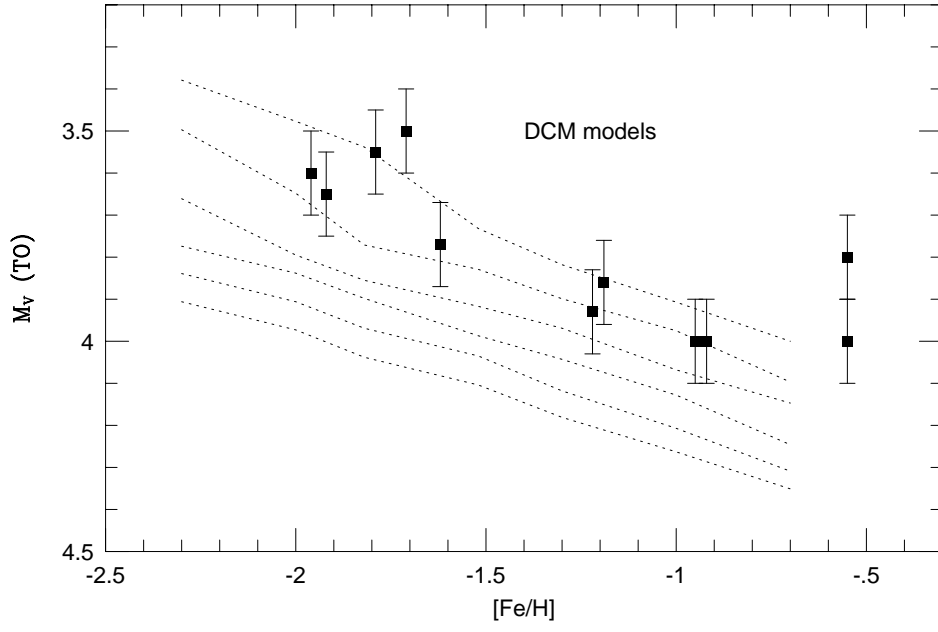


Fig. 9.—

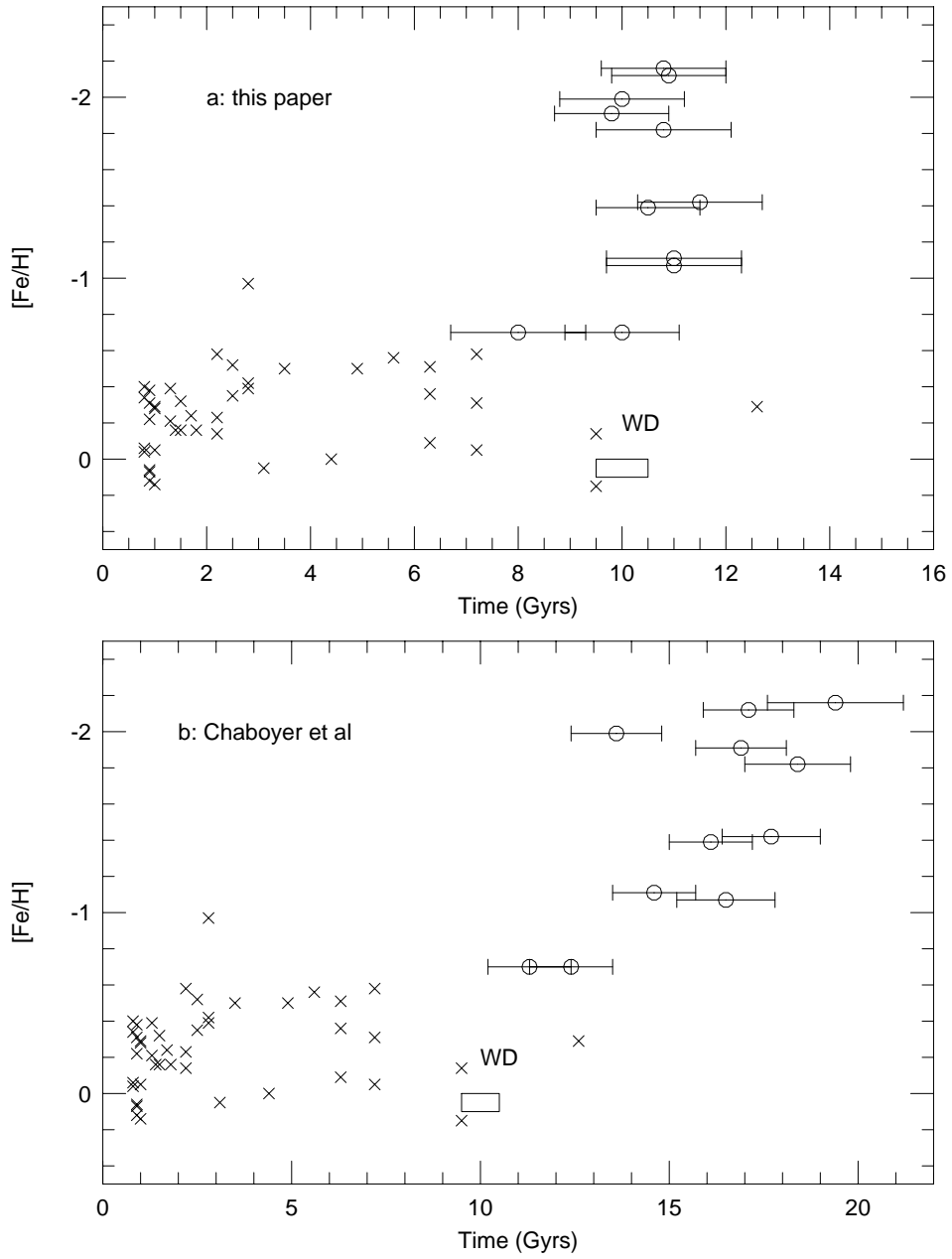


Fig. 10.—



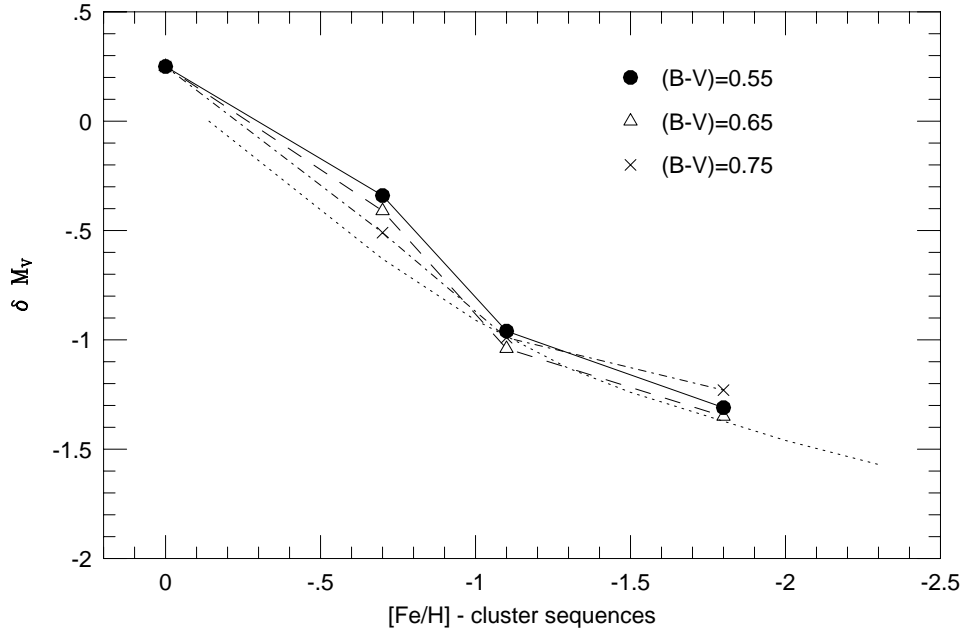


Fig. 11.—

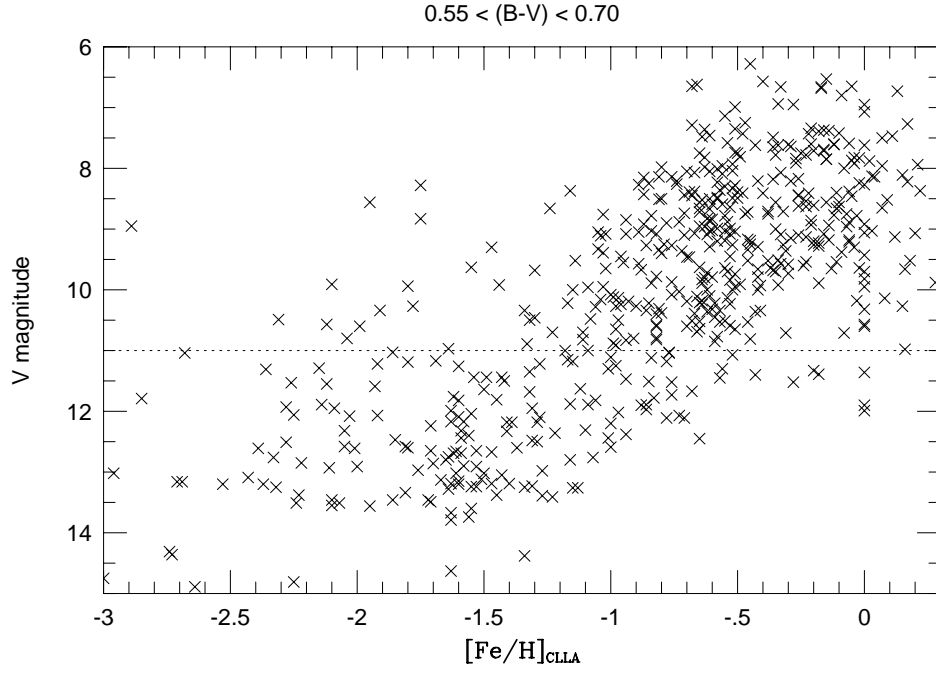


Fig. 12.—

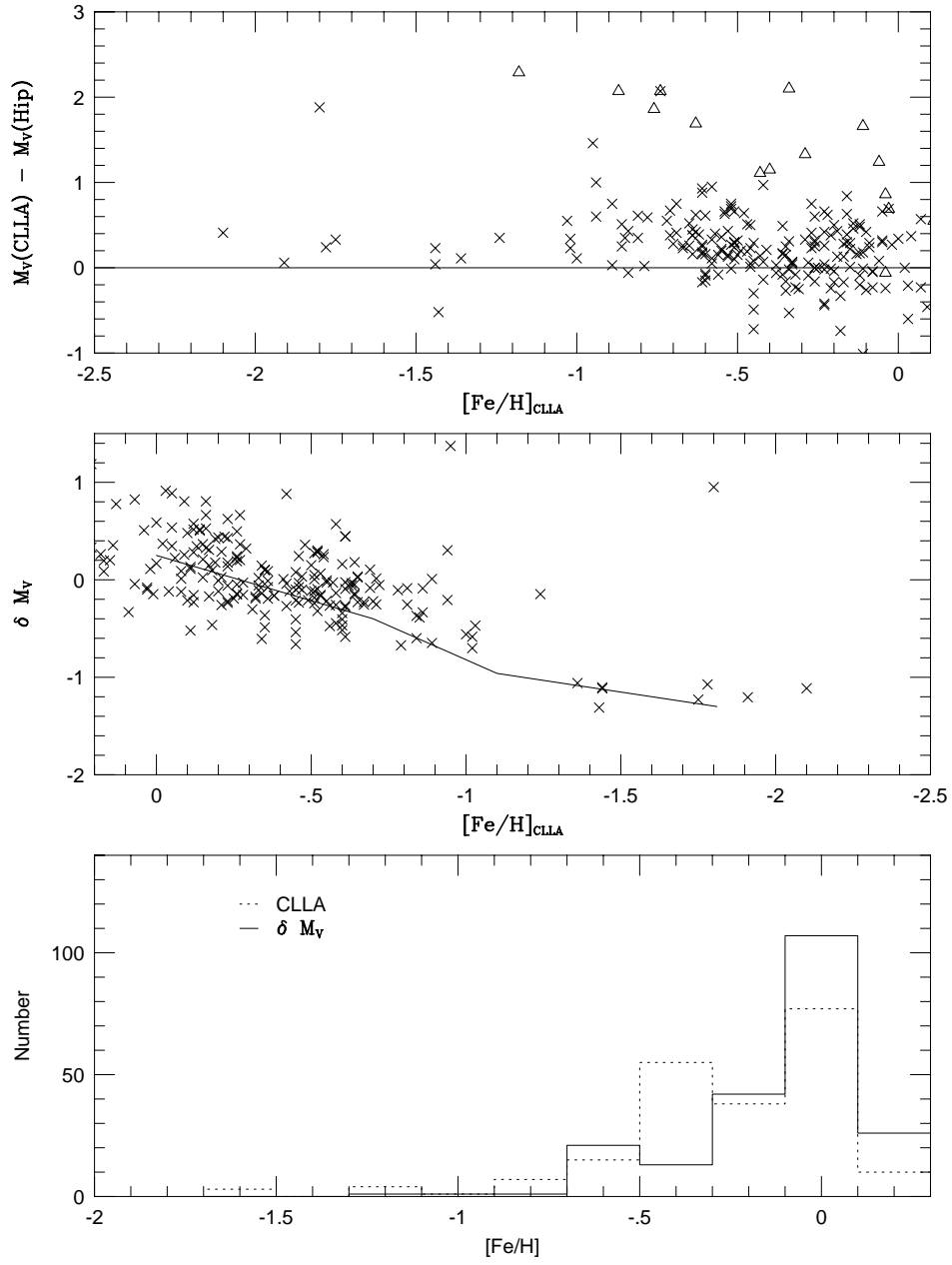


Fig. 13.—

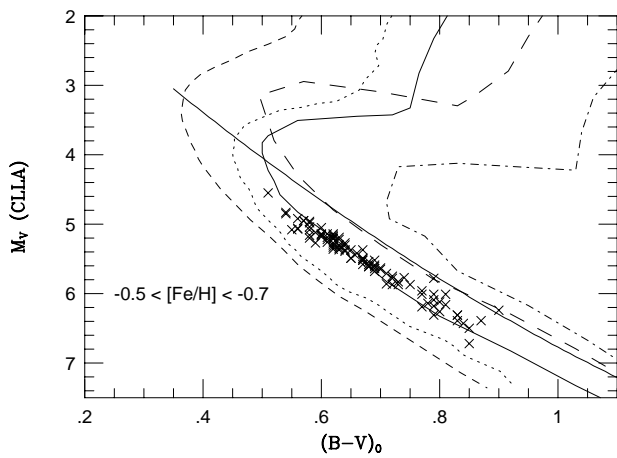
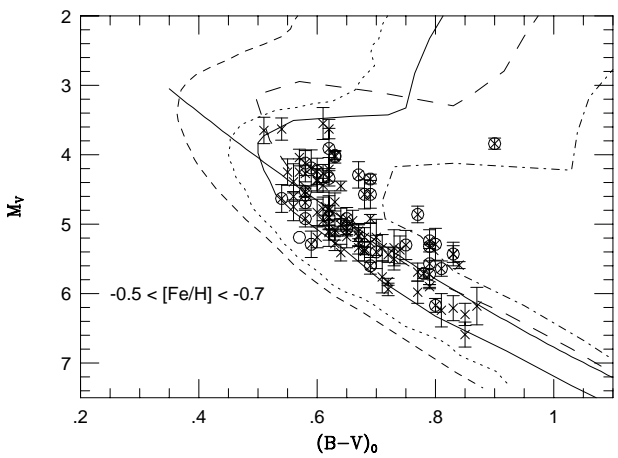
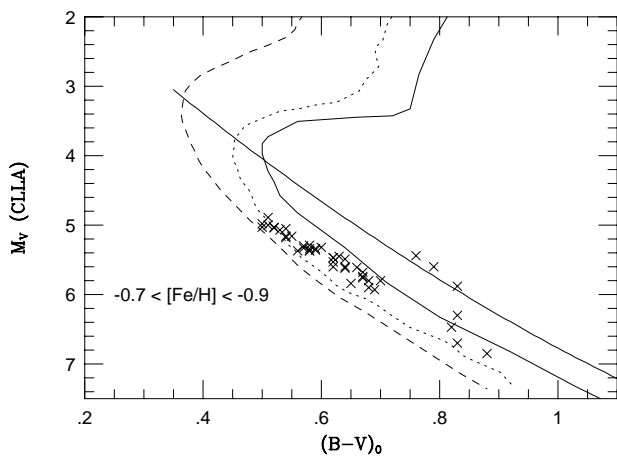
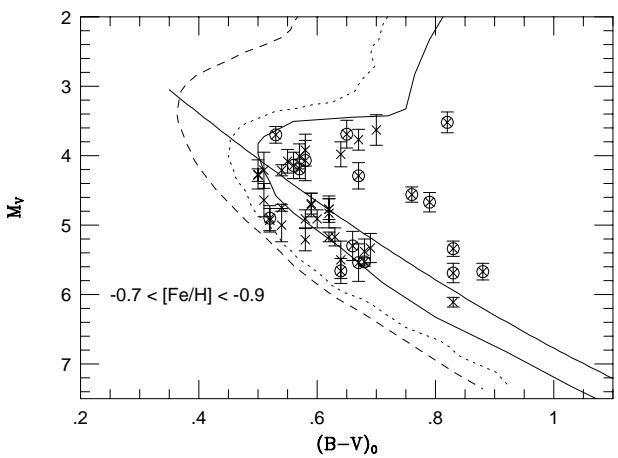
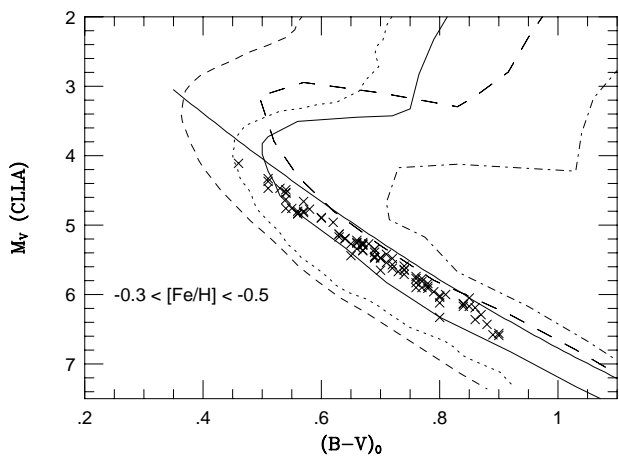
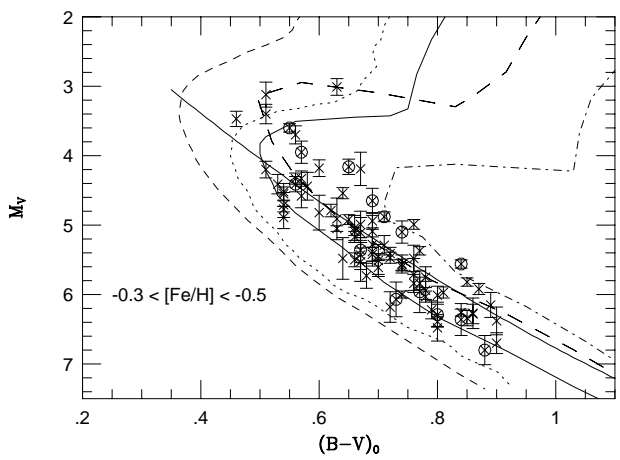


Fig. 14.—

Fig. 14.—



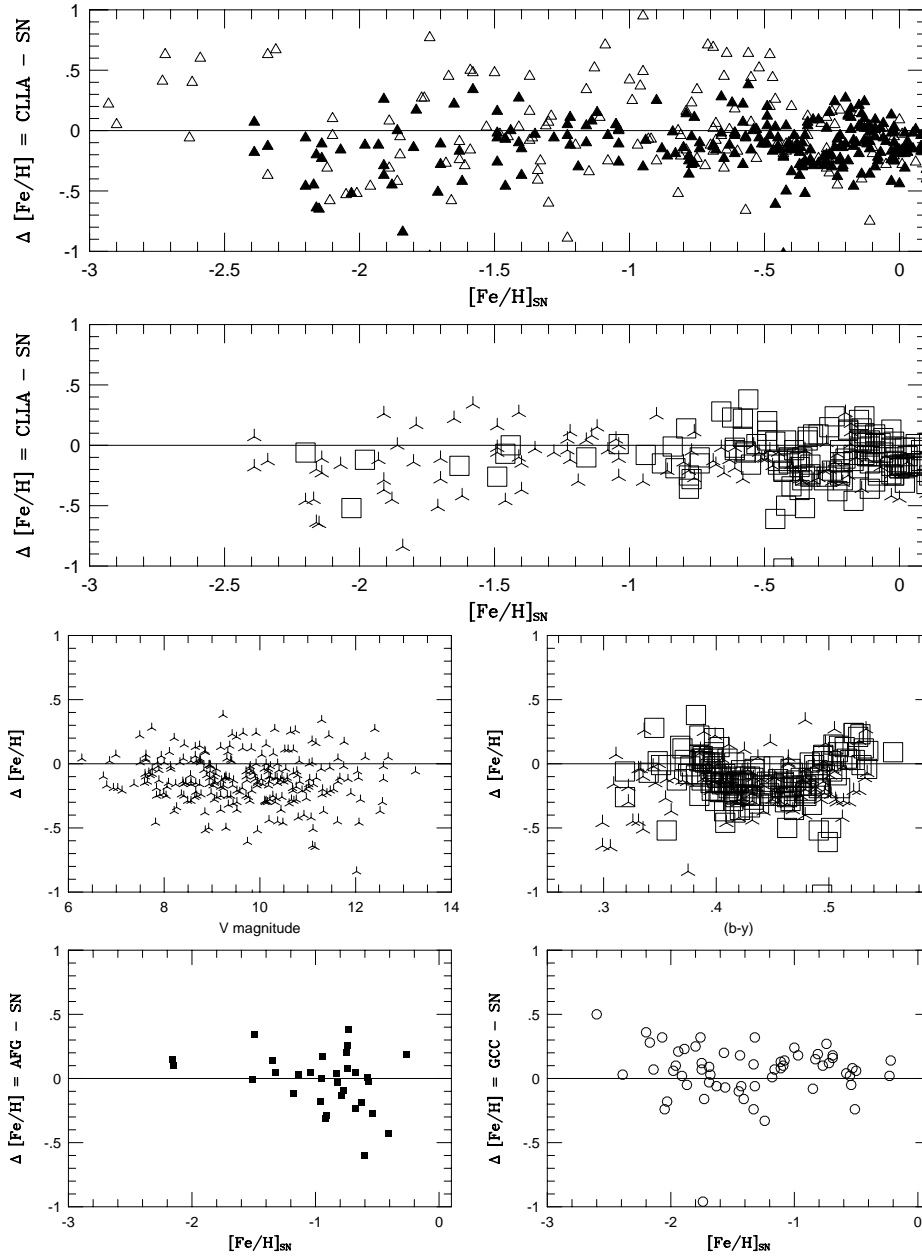


Fig. 15.—

Fig. 16.—

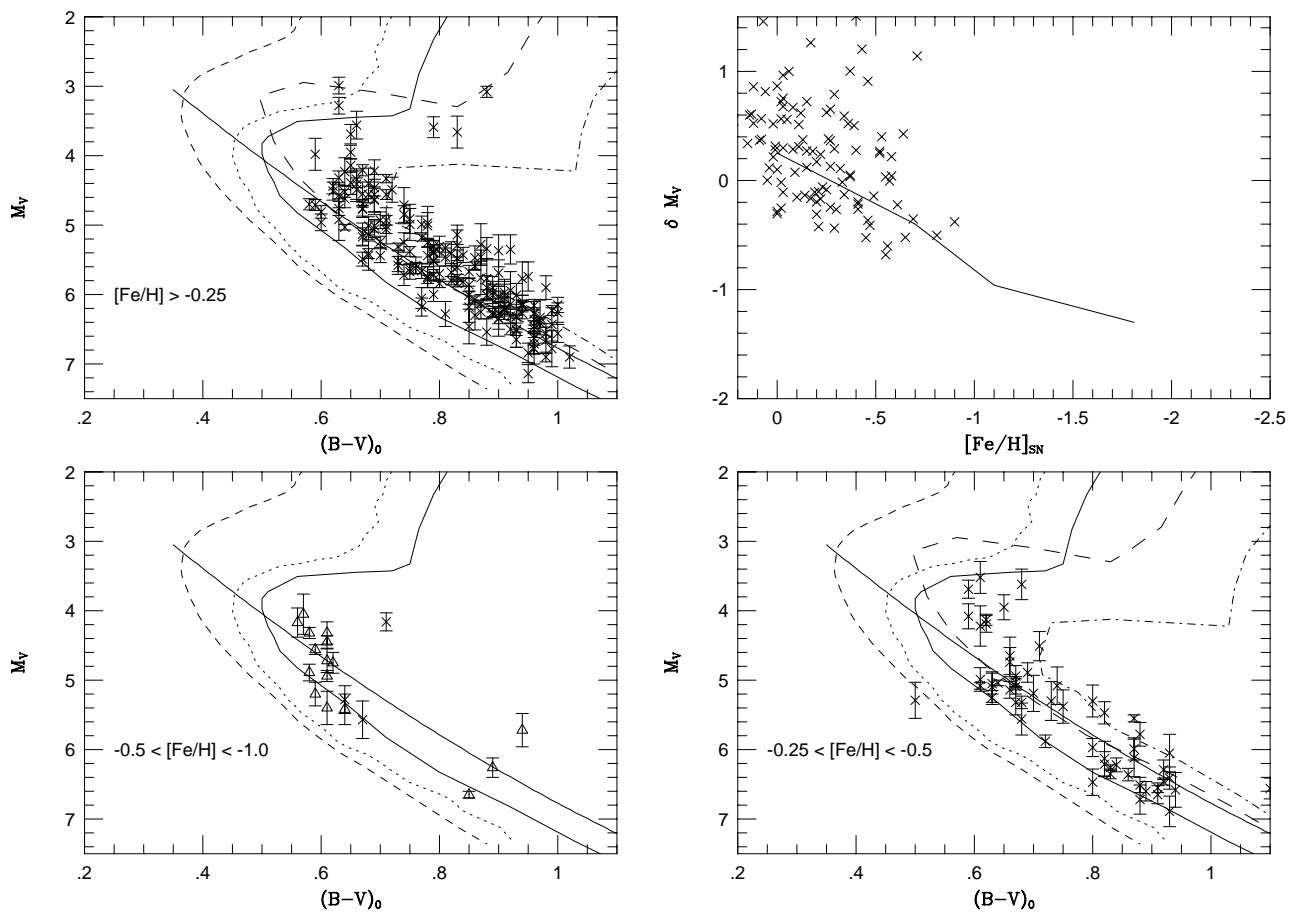


TABLE 1. The local calibrators

HIC	$V_0$	$(B-V)_0$	$M_V$	$M_V^{LK}$	$\frac{\sigma_\pi}{\pi}$	[Fe/H]	Source	name	
2319	7.62	0.47	3.22	3.18	0.070	-0.54	GCC	HD 2615	
3026	9.25	0.46	4.15	3.97	0.144	-1.17	GCC	HD 3567	G270-23
5336 <sup>1</sup>	5.17	0.70	5.78	5.78	0.005	-0.86	AFG	HD 6582	$\mu$ Cas
5862	4.97	0.57	4.08	4.08	0.010	0.09	GCC	HR 370	
6159 <sup>2</sup>	8.90	0.59	4.77	4.72	0.082	-0.82	AFG	HD 7983	G271-34
7869 <sup>3</sup>	8.33	0.54	4.06	4.04	0.053	-1.14	AFG	HD 10607	LHS 1281
	12.44	1.21	8.17	8.15	0.053	-1.14	AFG	LHS 1279	cpm to HD 10607
10140 <sup>4</sup>	8.76	0.57	4.99	4.95	0.073	-0.99	AFG	BD+29 366	G74-5
10449	9.08	0.57	5.12	5.07	0.083	-0.77	AFG	BD-01 306	G159-50
12579 <sup>5</sup>	9.16	0.52	4.97	4.91	0.088	-0.78	AFG	BD+46 610	G78-1
14594	8.04	0.45	5.10	5.09	0.044	-1.89	GCC	HD 19445	G37-26
15371 <sup>6</sup>	5.24	0.60	4.83	4.83	0.006	-0.24	GCC	HR 1010	$\zeta^2$ Ret
16404 <sup>7</sup>	9.91	0.65	6.14	6.08	0.087	-1.92	GCC	BD+66 0268	G246-38
17147	6.68	0.54	4.75	4.75	0.021	-0.76	GCC	HD 22879	G80-15
18915	8.51	0.86	7.18	7.18	0.020	-1.69	GCC	HD 25329	
19797	9.23	0.36	4.77	4.68	0.104	-1.57	GCC	HD 284248	G8-16
22596 <sup>8</sup>	6.94	0.56	4.56	4.55	0.033	-0.46	GCC	HD 30649	
24316	9.43	0.50	5.24	5.20	0.069	-1.44	GCC	HD 34328	
31188	8.60	0.56	4.73	4.70	0.058	-0.81	AFG	HD 46341	
33221	9.07	0.48	3.87	3.77	0.111	-1.33	GCC	CD-33 3337	
36491	8.48	0.52	4.99	4.94	0.083	-1.02	AFG	HD 59374	G88-31
38541 <sup>9</sup>	8.27	0.61	6.01	6.00	0.029	-1.60	GCC	HD 64090	G90-25
38625 <sup>10</sup>	7.43	0.73	6.01	6.00	0.036	-0.93	GCC	HD 64606	G112-54
40613	7.74	0.58	4.29	4.26	0.057	-0.55	GCC	HD 69611	G113-24
40778	9.73	0.48	4.81	4.64	0.142	-1.49	GCC	BD+54 1216	G194-22
42734	7.42	0.58	4.08	4.07	0.044	-0.57	GCC	HD 74011	
44811	7.72	0.57	4.72	4.71	0.027	-0.62	GCC	HD 78747	
47139	8.33	1.01	-0.21	-5.06	0.500	-1.51	GCC	HD 83212	
48113	5.08	0.62	3.75	3.75	0.014	0.07	GCC	HR 3881	
48152 <sup>a</sup>	8.33	0.40	3.80	3.74	0.085	-2.07	GCC	HD 84937	G43-3
49793	8.07	0.59	4.78	4.77	0.041	-0.66	AFG	HD 88261	
50384 <sup>11</sup>	5.81	0.50	4.03	4.03	0.017	-0.38	GCC	HR 4039	
51415	9.04	0.56	5.28	5.26	0.053	-1.01	AFG	HD 91345	
51700	7.50	0.56	4.72	4.71	0.030	-0.45	GCC	HD 91347	
53070 <sup>a</sup>	8.21	0.47	4.63	4.60	0.059	-1.38	GCC	HD 94028	G58-25
54641	8.16	0.48	4.41	4.40	0.043	-1.04	AFG	HD 97320	
55790	9.07	0.48	4.27	4.12	0.135	-1.56	AFG	HD 99383	
56837	8.45	0.69	5.59	5.58	0.040	-0.40	AFG	BD+45 1949	G122-39
57360	8.75	0.43	4.23	4.16	0.096	-1.20	AFG	HD 102200	
57450	9.91	0.55	5.58	5.48	0.113	-1.26	GCC	BD+51 1696	G176-53
57939	6.42	0.75	6.61	6.61	0.007	-1.22	GCC	HD 103095	G122-51
59699	9.28	0.57	4.14	4.00	0.130	-0.75	AFG	HD 106411	
60551 <sup>a</sup>	8.03	0.57	5.18	5.17	0.030	-0.75	AFG	BD+39 2519	G123-2



TABLE 1. (continued)

HIC	$V_0$	$(B-V)_0$	$M_V$	$M_V^{LK}$	$\frac{\sigma_\pi}{\pi}$	[Fe/H]	Source	name	
60632	9.66	0.44	4.86	4.75	0.118	-1.55	GCC	HD 108177	G13-35
60779	9.28	0.58	4.85	4.76	0.103	-0.60	AFG	HD 108405	
62207	5.95	0.56	4.75	4.75	0.011	-0.51	GCC	HR 4845	
62923 <sup>12</sup>	8.02	0.51	3.95	3.87	0.102	-0.55	AFG	HD 111971	
64426	7.30	0.52	4.26	4.23	0.058	-0.67	GCC	HD 114762	
65201 <sup>13</sup>	8.80	0.45	4.76	4.69	0.093	-1.86	GCC	HD 116064	
66509	8.81	0.68	5.20	5.17	0.064	-0.59	AFG	HD 118659	G63-44
68246	8.61	0.42	3.38	3.29	0.107	-0.66	AFG	HD 121387	
68464	8.73	0.46	3.68	3.53	0.135	-1.75	GCC	HD 122196	
70520	7.27	0.58	3.91	3.90	0.039	-0.56	GCC	HD 126512	
71284 <sup>14</sup>	4.47	0.36	3.52	3.52	0.011	-0.41	GCC	HR 5447	
72461 <sup>15</sup>	9.73	0.43	4.79	4.63	0.138	-2.29	GCC	BD+26 2606	G166-45
72673	7.16	0.45	3.76	3.75	0.042	-0.55	GCC	HD 130551	
74079	7.67	0.56	3.80	3.77	0.066	-0.72	GCC	HD 134169	
74234 <sup>16</sup>	9.44	0.85	7.08	7.06	0.050	-1.57	GCC	HD 134440	
74235 <sup>16</sup>	9.07	0.77	6.74	6.73	0.040	-1.57	GCC	HD 134439	
76976	7.20	0.48	3.41	3.39	0.056	-2.38	GCC	HD 140283	
77760	4.60	0.56	3.60	3.60	0.009	-0.46	GCC	HR 5914	
80587	7.69	0.55	4.08	4.06	0.052	-0.61	GCC	HD 148211	
80837	7.27	0.54	4.20	4.19	0.037	-0.68	GCC	HD 148816	G17-21
84862 <sup>17</sup>	5.38	0.62	4.59	4.59	0.008	-0.38	GCC	HR 6458	
84905	6.95	0.57	4.01	4.00	0.037	-0.51	GCC	HD 157089	
85373 <sup>18</sup>	9.67	0.82	5.41	5.35	0.089	-0.63	AFG	HD 158226B	
85378 <sup>18</sup>	8.48	0.61	4.29	4.26	0.064	-0.63	AFG	HD 158226A	G181-47
86013 <sup>19</sup>	8.37	0.58	4.97	4.95	0.056	-1.08	AFG	BD+06 3455	G139-48
86694	8.72	0.46	3.41	3.23	0.144	-1.73	GCC	HD 160617	
88622	6.80	0.61	4.86	4.86	0.021	-0.44	GCC	HD 165401	
88745 <sup>20</sup>	5.05	0.53	4.08	4.08	0.009	-0.54	GCC	HR 6775	HD 165908
89554	8.22	0.44	4.25	4.22	0.065	-1.44	GCC	HD 166913	
92532	7.15	0.54	4.76	4.76	0.018	-0.46	GCC	HD 174912	G207-5
96185	6.62	0.60	4.10	4.10	0.020	-0.53	GCC	HD 184499	
98020	8.83	0.59	5.85	5.83	0.046	-1.37	GCC	HD 188510	G143-17
99267	10.11	0.51	5.51	5.44	0.094	-2.01	AFG	BD+42 3607	G125-64
100568	8.65	0.55	5.45	5.43	0.054	-1.00	GCC	HD 193901	
100792	8.33	0.49	4.60	4.56	0.069	-1.03	GCC	HD 194598	G24-15
102862	8.94	0.63	5.06	5.01	0.077	-0.48	AFG	HD 198245	
103269	10.28	0.62	6.05	5.96	0.103	-1.60	AFG	BD+41 3931	G212-7
104659	7.37	0.52	4.63	4.62	0.036	-0.94	GCC	HD 201891	
105858	4.21	0.49	4.39	4.39	0.005	-0.62	GCC	HR 8181	HD 203608
105888	8.49	0.57	4.06	4.00	0.085	-1.01	AFG	BD+04 4674	G25-49
106749	9.04	0.53	5.39	5.36	0.066	-1.21	AFG	HD 205650	
107975	5.52	0.43	3.31	3.31	0.019	-0.59	GCC	HR 8354	HD 207978
108490 <sup>21</sup>	6.95	0.50	4.62	4.62	0.021	-0.65	GCC	HD 208906	
112229	7.41	0.50	4.28	4.27	0.041	-0.62	GCC	HD 215257	
112447 <sup>22</sup>	4.20	0.50	3.15	3.15	0.013	-0.30	GCC	HR 8665	

TABLE 1. (continued)

HIC	$V_0$	$(B-V)_0$	$M_V$	$M_V^{LK}$	$\frac{\sigma_{\pi}}{\pi}$	[Fe/H]	Source	name
112935	5.16	0.49	3.02	3.02	0.020	-0.23	GCC	HR 8697
113357	5.45	0.67	4.52	4.52	0.012	0.08	GCC	HR 8729
116771 <sup>23</sup>	4.13	0.51	3.43	3.43	0.012	-0.17	GCC	HR 8969

<sup>1</sup>CCDM J0108+5455,  $V \sim 11$  M-dwarf companion

<sup>2</sup>CCDM J01191-0856,  $m_1=9.3$ ,  $m_2=10.8$ , omitted from MS fitting

<sup>3</sup>CCDM J01412-6741, companion is LHS 1279,  $\Delta m = 4$  mag

<sup>4</sup>CCDM J02104+2948,  $\Delta m = 4$  mag

<sup>5</sup>SB1 CLLA, omitted from MSF

<sup>6</sup>CCDM J03180-6232, wide cpm companion of  $\zeta^1$  Ret

<sup>7</sup>Suspected as not single from Hipparcos astrometry, omitted from MS fitting

<sup>8</sup>CCDM J04518+4550, optical companion?,  $\Delta m = 5$  mag

<sup>9</sup>CCDM J07536+3037, SB1? CLLA, optical comp.  $\Delta m = 5$  mag

<sup>10</sup>CCDM J07546-0215, SB1 CLLA, omitted from MS fitting

<sup>11</sup>CCDM J10172+2306, Gl 387AB,  $\Delta m = 5$  mag

<sup>12</sup>CCDM J12590-0950,  $m_1=8.7$ ,  $m_2=9.3$ . omitted from MS fitting

<sup>13</sup>CCDM J13217-0950, no data on companion

<sup>14</sup>CCDM J14347+2945, two optical(?) companions, both  $\Delta m > 5$  mag

<sup>15</sup>SB1 CLLA, omitted from MS fitting

<sup>16</sup>CCDM J15102-1624, wide well-resolved binary

<sup>17</sup>CCDM J17206+3229, two optical(?) companions, both  $\Delta m > 4.5$  mag

<sup>18</sup>CCDM J17267+3104, wide well-resolved binary

<sup>19</sup>CCDM J17348+0601, ADS 10638C, wide well-resolved binary

<sup>20</sup>CCDM J18071+3034, Gl 704,  $\Delta m = 3.5$  mag

<sup>21</sup>CCDM J21547+2949, optical(?) companion,  $\Delta m > 6.5$  mag

<sup>22</sup>CCDM J22467+1211, optical(?) companions,  $\Delta m > 7$  mag

<sup>23</sup>CCDM J23399+0538, optical(?) companion,  $\Delta m > 8$  mag

<sup>a</sup>Suspected single-lined binary, CLLA. Omitted from MS fitting

TABLE 2. Main-sequence fitting distance moduli to globular cluster

cluster	$E_{B-V}$	[Fe/H]	$(m-M)_0^{LK}$	$(m-M)_0$	$N_{ref}$	$[Fe/H]_{lim}$
NGC 6397	0.19	-1.82	12.25	12.24	8	-1.5 to -2.05
NGC 6752	0.04	-1.42	13.17	13.16	12	-1.2 to -12.7
M13	0.02	-1.39	14.45	14.45	9	-1.15 to -1.65
M5	0.02	-1.10	14.53	14.52	9	-0.9 to -1.35
NGC 288	0.01	-1.07	15.00	15.00	9	-0.85 to -1.30
M71	0.28	-0.70	13.20	13.19	9	-0.45 to -0.90
47 Tuc	0.04	-0.70	13.57	13.56	9	-0.45 to -0.90

TABLE 3. Proper-motion star samples : Apparent magnitude distributions

V mag.	A	B	C	D	E
6.25		1		1	2
6.75		14		13	18
7.25		18		18	39
7.75		38		38	73
8.25	2	49	2	48	102
8.75	5	52	3	45	84
9.25	6	53	5	43	98
9.75	9	43	6	33	76
10.25	10	37	9	19	39
10.75	9	28	3	9	20
11.25	18	14	9	2	14
11.75	19	11	6	1	6
12.25	22	7	2		3
12.75	27	1			
13.25	33				
13.75	8				
14.25	3				
14.75	4				

## Notes to Table 3.

Apparent magnitude distributions for five subsets of Lowell proper-motion stars with (B-V) colours in the range 0.55 to 0.70 magnitudes:

- A. CLLA stars with  $[\text{Fe}/\text{H}] < -1$ ;
- B. CLLA stars with  $[\text{Fe}/\text{H}] \geq -1$ ;
- C. CLLA stars with  $[\text{Fe}/\text{H}] < -1$  and Hipparcos parallax measurements;
- D. CLLA stars with  $[\text{Fe}/\text{H}] \geq -1$  and Hipparcos parallax measurements;
- E. the full Hipparcos sample.